Aus dem Department für Zahn-, Mund- und Kieferheilkunde
Klinik für Zahn-, Mund und Kieferheilkunde
der Albert-Ludwigs-Universität Freiburg im Breisgau

Accuracy of computerized and conventional impression-making procedures of straight and tilted dental implants

INAUGURAL – DISSERTATION

zur

Erlangung des Zahnmedizinischen Doktorgrades
der Medizinischen Fakultät
der Albert-Ludwigs-Universität
Freiburg im Breisgau

Vorgelegt 2015

von Aiste Gintaute

geboren in Kaunas, Litauen

Dekanin:	Prof. Dr. Kerstin Krieglstein
1. Gutachter:	Prof. Dr. Wael Att
2. Gutachter:	Prof. Dr. Karl-Thomas Wrbas
Jahr der Promotion:	2016

List of abbreviations

3D	Three-dimensional
CAD/CAM	Computer-aided design/ Computer-aided manufacture
CAI	Computer-aided impression
CMM	Coordinate measuring machine
CMOS	Complementary metal-oxide semiconductor
D	Diameter
IA	Implant analog
IOS	Intraoral scanner
P	Emergence profile
PEEK	Polyether ether ketone
RM	Reference model
SD	Standard deviation
STL	Standard Tessellation Language
VPS	Vinyl polysiloxan

Table of Contents

1 Introduction

Over the past 40 years, treatment strategies for fully and partially edentulous patients have improved remarkably. Changes in treatment possibilities began in 1952 with the discovery of the osseointegration process by Prof. Per-Ingvar Brånemark; in 1978, the insertion of implants was approved for clinical purposes (Adell, Lekholm, Rockler, & Branemark, 1981; Branemark et al., 1977).

There are three main causes of tooth loss: caries, periodontal disease, and trauma. Despite many improvements in dental care in the last decades, a surprisingly high number of patients still suffers from edentulism. A recent population-based study of tooth loss in the US showed that 14.3% of US adults (74.8% <65 years old, 25.2% ≥65 years old) had all of their teeth removed and were fully edentulous (Saman, Lemieux, Arevalo, & Lutfiyya, 2014). Furthermore, it was found 22.6% of the German population between 65-70 years to be completely edentulous as well (Micheelis & Schiffner, 2006).

Each tooth loss evokes alveolar bone atrophy with a different severity, which increases over time (Patzelt, Bahat, Reynolds, & Strub, 2014). Tooth loss in an edentulous jaw can be prosthetically restored in three different manners: with complete dentures, removable implant-retained prostheses, and fixed implant-supported prostheses (Att, Bernhart, & Strub, 2009). However, the esthetic and functional demands of patients nowadays are very high. Implant-retained or supported prostheses are one of the most favorable treatment options for edentulous patients. They are especially advantageous in the lower jaw, where severe alveolar ridge atrophy leads to an unstable complete denture and constant discomfort for a patient. Nevertheless, implant placement in such cases can be also complicated by insufficient bone support, usually in posterior regions of a mandible, which may require a bone augmentation procedure. Alternatively, existing bone might be utilized using shorter or angled implants or implanting only in the areas where the amount of bone is sufficient.

One of the most popular concepts presented for lower jaw reconstructions was published more than a decade ago (Malo, Rangert, & Nobre, 2003). It was suggested to place four interforaminal implants without invasive bone regeneration procedure in the posterior segments. Two middle implants should to be positioned axially and two lateral implants distally angled. In such cases, the definitive reconstruction could be manufactured either as a removable or fixed prosthesis, since the angled implants ensure a minimized cantilever length. In contrast, if all four implants were placed axially, a removable implant-retained dental prosthesis would be preferable.

In order to fabricate a prosthetic framework on multiple implants, high-precision clinical and laboratory procedures are required. Today, for almost every step in the procedure, either conventional or computer-aided approaches can be utilized. Regardless of the approach, the major goal is to provide a restoration with a passive fit.

1.1 Passive fit of multiple implant restorations

The fabrication of an implant-borne superstructure that passively fits is fundamentally important. One of the reasons is the variable load transfer pattern on teeth and implants. Teeth are able to move 25-100 µm axially and 56-108 µm laterally (Y. Kim, Oh, Misch, & Wang, 2005; Schulte, 1995). This motion is particularly affected by existing periodontal ligaments and explains why natural teeth are prone to migrate under the overload. Implants, on the other hand, might generate only 3-5 µm axial and 10-50 µm lateral movements (Y. Kim et al., 2005; Schulte, 1995). The load on implants is transferred directly to the bone, mainly on the crest (Richter, 1998). Non-passively fitting implant reconstructions generate internal stress upon loading, which may affect the bone-implant interface (Sahin, Cehreli, & Yalcin, 2002). Over time, this could lead to biological and technical complications. Additionally, screw loosening or fracture of the implant or prosthesis might lead to compromised implant longevity (Schwarz, 2000). It could also induce pain, tenderness, marginal bone loss, or loss of osseointegration (Kan, Rungcharassaeng, Bohsali, Goodacre, & Lang, 1999). It seems, however, that biology can tolerate some degree of misfit, but it is not clear to what extent (Katsoulis, Muller, Mericske-Stern, & Blatz, 2015). Nevertheless, there are no longitudinal studies, to our knowledge, that would specifically attribute implant failures only to framework misfit. Moreover, the absolute passive fit practically does not exist and cannot be achieved (Lin, Harris, Elathamna, Abdel-Azim, & Morton, 2015; Sahin & Cehreli, 2001). Even though the clinicians should seek the best possible implant reconstruction fit, it remains unclear what level of misfit is clinically acceptable. However, it has been suggested that an acceptable machining tolerance has a range between 22 and 100 µm (Ma, Nicholls, & Rubenstein, 1997). Some studies adhere to the same limitation (Katsoulis et al., 2015) and some, though, publish a higher reasonable mismatch of 150 µm (Jemt, 1991).

It was stated that the clinical procedures applied for a misfit evaluation are based on the tactile and visual senses of a human and can hardly be calibrated (Tan, Rubenstein, Nicholls, & Yuodelis, 1993). Nevertheless, several methods were suggested to assess the fit of the framework on implants, e.g. alternate finger pressure, direct vision and tactile sensation, radiographs, one screw test (Sheffield test), screw resistance test, disclosing media, and three dimensional quantifying systems

(Kan et al., 1999). However, each of these methods is associated with a certain degree of subjectivity and complexity; therefore, a combination of the available tests is strongly recommended.

1.2 Conventional approach

Conventional procedures and materials have been widely discussed in the literature and applied for years in routine dental practice. However, every conventional step (impression material, impression procedure, fabrication of master cast, wax pattern, framework, and definitive prosthesis) generates a certain amount of error and cannot be fully automated (Carr & Stewart, 1993; Del Corso, Aba, Vazquez, Dargaud, & Dohan Ehrenfest, 2009). Each introduced error, though, can be either accumulated or compensated, leading to the so called “distortion equation” phenomenon, which theoretically assures an accurate final restoration (Wee, Aquilino, & Schneider, 1999).
Furthermore, conventional procedures with implants are even more complex than with teeth. This is due to the additional components used to facilitate the transfer of the three-dimensional implant position from the mouth to the cast. Each component connected to the implant or abutment, and later to the implant- or abutment-analog, has a proper machining tolerance (S. Kim, Nicholls, Han, & Lee, 2006). The machining tolerance can be considered an additional source of error and can not exceed aforementioned machining tolerance of 22-100 µm (Ma et al., 1997), which is believed to be clinically acceptable.

Moreover, if the implants are tilted at different angles, performing a highly accurate conventional impression may be challenging. The usual reason for this is the distortion of the impression material, i.e. the elastic recovering potentiality is exceeded within the highly applied forces during the disconnection and removal of the impression (Mpikos et al., 2012). Nevertheless, there is no unanimous scientific agreement regarding which quantity and angulation of implants causes non-compensated impression material distortions, and when they must be splinted.
The accuracy of splinted and non-splinted open-tray implant impressions was compared in the *in vivo* study (S. Kim et al., 2006). Five parallel implants were placed in a mandible and a light curing resin was used to block the implants. The authors concluded that three-dimensional linear distortions of the non-splinted implant impression group were smaller than distortions in the splinted group. However, the splinted group showed better results during fabrication of the definitive casts. Nevertheless, if the entire amount of displacement from the impression-making procedure to the definitive cast fabrication was considered, no significant difference was found between both groups.

Another study tested the accuracy of splinted and non-splinted implant impressions of 5 mandibular implants (Burawi, Houston, Byrne, & Claffey, 1997). It was concluded that the splinted technique results in a higher mean deviation anterior-to-posterior (-0.526 mm) than the non-splinted technique (0.0434 mm).
Despite the aforementioned studies, there are many other studies in the literature that recommend splinting implants before making an impression (de Avila, de Matos Moraes, Castanharo, Del'Acqua, & de Assis Mollo, 2014; Faria, Silva-Concilio, Neves, Miranda, & Teixeira, 2011; Hariharan, Shankar, Rajan, Baig, & Azhagarasan, 2010; Martinez-Rus, Garcia, Santamaria, Ozcan, & Pradies, 2013; Ongul, Gokcen-Rohlig, Sermet, & Keskin, 2012; Pujari, Garg, & Prithviraj, 2014; Yamamoto, Marotti, de Campos, & Neto, 2010; Zen et al., 2014). A recent systematic review included 76 studies and showed a clear tendency for the splinted impression technique to be more accurate (Papaspyridakos et al., 2014). However, shrinkage of the splinting material remains a common problem. The most frequently used splinting material is an auto-polymerizing acrylic resin (Pozzi, Tallarico, Mangani, & Barlattani, 2013). It contracts volumetrically between 6.5 and 7.9% in the first 24 hours, with 80% of shrinkage in the first 17 minutes after mixing (Mojon, Oberholzer, Meyer, & Belser, 1990). Other materials, such as bis-acrylic resin (Zen et al., 2014), light-polymerizing acrylic resin (Rutkunas & Ignatovic, 2014), bite registration addition silicone or bite registration polyether (Hariharan et al., 2010), and metal or prefabricated resin burs (de Avila et al., 2014; Del Acqua, Chavez, Castanharo, Compagnoni, & Mollo Fde, 2010; Filho, Mazaro, Vedovatto, Assuncao, & dos Santos, 2009) are suggested as alternatives.

There is also no general agreement in the literature about which implant impression method is more advantageous. However, both types (direct open-tray and indirect closed-tray) of implant impression are widely discussed in the literature. An *in vitro* study found no difference between the direct open-tray and indirect closed-tray impressions (Wenz & Hertrampf, 2008).
Another study, however, concluded that the difference between direct and indirect impression making methods of the reference model with five mandibular implants is statistically significant (Carr, 1991). In this study, the most accurate working cast was produced using the direct transfer method. The inaccuracies of the indirect method correlated with the non-parallel implant position (<15˚) and the deformation of the impression material.
Likewise, a systematic review reported that more studies confirm a higher impression accuracy (for four or more implants) using an open-tray impression technique than a closed-tray method (H. Lee, So, Hochstedler, & Ercoli, 2008). Additionally, polyether and PVS were recommended as

statistically the most accurate materials to perform a precise open-tray implant impression (Wee, 2000).

In summary, the accuracy of the conventional implant impression-making procedure is a critical factor that can significantly influence the quality and fit of the restoration onto the dental implants and which could be alternatively substituted with computer-aided impression making methods.

1.3 Computer-aided approach

Over the past few years, digital technologies have developed rapidly. This obviously influenced existing transformations in the science, industry, and daily life. Together with progressive changes in three-dimensional technologies, new inventions also appeared in dental medicine; these major breakthroughs led to the development of CAD/CAM (Computer-aided design/Computer-aided manufacture) technologies.

Starting with the first computer-aided approach in restorative dentistry in the late 1980s (Lutz, Krejci, & Mormann, 1987; Mormann & Brandestini, 1987; Mormann, Brandestini, & Lutz, 1987), advances in data acquisition, processing, and manufacturing nowadays afford much faster and more accurate final outcomes. The introduction and development of various intraoral scanners (IOS) led to their popularity and extensive application in dental medicine. Most IOSs are based on non-contact reflective optical technologies represented by confocal microscopy, optical coherence tomography, active and passive stereovision and triangulation, interferometry, and phase shift principles (Logozzo, Zanetti, Franceschini, Kilpelä, & Mäkynen, 2013).

Every IOS system has the same three principles (digitation, generalization/fusion, and optimization), which lead to a digital reconstruction of the three-dimensional object. First of all, the object is visible as a point cloud in which each point has its own x-, y-, and z-coordinates. Next, during stitching and overlapping of the different digital images, these points are connected into triangles. Following this, polygon meshes are formed, and the triangles are filled in. In this way, the clouds of points become clear recognizable objects (Figure 1-1).

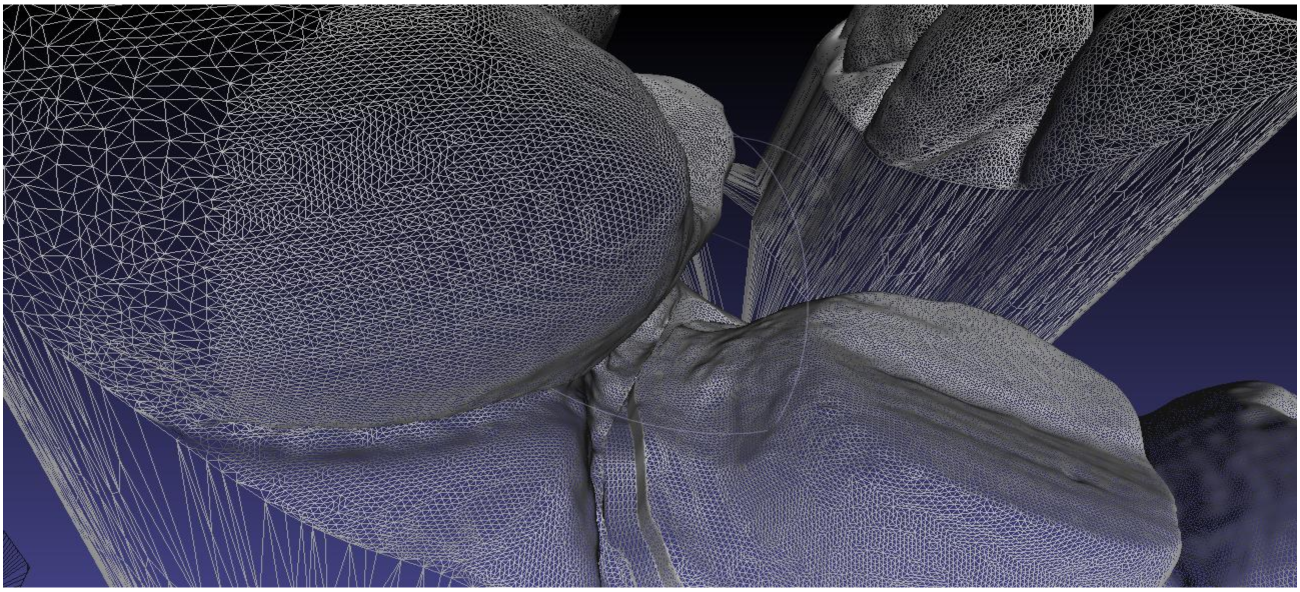

Courtesy of 3M ESPE Germany GmbH

Figure 1-1: Illustration of the polygon meshes formed during the digital 3D object reconstruction process.

However, a certain probability of error also exists in every three-dimensional object reconstruction process. This error can manifest due to insufficient point sampling density, misalignment of the point clouds, data outliers, data noise, or missing data. The source of these errors might be: non- or poorly-calibrated scanning devices or scanning technology (Patzelt, Emmanouilidi, Stampf, Strub, & Att, 2014), operator inexperience (Dehurtevent, Robberecht, & Behin, 2015; Gimenez, Ozcan, Martinez-Rus, & Pradies, 2013), hand shaking or incorrect IOS wand position relative to the object (Mada, Smith, Smith, & Midha, 2003), incorrect scanning method (Ender & Mehl, 2013b), patient movements, improper scanning powder application (Ender & Mehl, 2013b; J. H. Kim et al., 2015), or the presence of saliva on the scanning surface.

However, the recent overviews (Reich, Vollborn, Mehl, & Zimmermann, 2013; Zimmermann, Mehl, Mormann, & Reich, 2015) systemized the advantages of the digital workflow with different IOSs and compared them to conventional approaches:

1. Real-time imaging for a better detection of the critical impression details
2. Easy repeatability without replacing retraction cords
3. Selective impression-making of the areas with poor accessibility
4. Virtual cutting tool for inadequately scanned areas and the possibility to incorporate an additional selective scan
5. Color reproduction for a better recognition of the tooth and gingival structures
6. Chairside analysis of the performed preparations

7. Easy communication with the patient and dental technician
8. Chairside CAD/CAM option
9. Virtual fusion possibility of the intraoral scan and computer tomography/digital volume tomography or extraoral facescan
10. Possibility to monitor the follow-up of systematically performed intraoral scans over time
11. Conventional material savings
12. Non-complicated model archivability
13. No model deterioration
14. Simple device disinfection

Despite these advantages, the digital approach has its own limitations as well. First, a considerable financial investment is required to purchase an intraoral scanner. Secondly, the cooperating dental technician laboratory has to be able to manufacture the restoration with the proper CAD/CAM equipment. Third, it is crucial to apply the right intraoral scanning protocol and to accept the learning curve. An *in vitro* study (Ender & Mehl, 2013b) showed that full-arch scanning accuracy is dependent on the correct intraoral scanning procedure. Furthermore, the simulation of dynamic occlusion is not sufficiently developed in every digital system (Reich et al., 2013). Finally, different IOSs have disparate indications, but to date, there is no IOS capable of perfect accuracy relative to conventional impressions. For example, the digitization of the edentulous jaw or large edentulous areas is particularly problematic (Patzelt, Vonau, Stampf, & Att, 2013).

Various manufacturers of intraoral scanners declared myriad reliable indications in restorative, surgical dentistry, as well as in orthodontics. The IOS might be applied for: inlays, onlays, veneers, single crowns, bridges, post and core restorations, removable partial dentures, single and multiple implant restorations, surgical guides, mouth guards, clear aligners, laboratory orthodontic appliances, custom braces, indirect-bonding trays, models, and tooth shade measurements. Still, not all indications and IOSs have been scientifically proven to be accurate alternatives to the conventional approach.

Today, many different intraoral scanners are available on the market and the current examples were published in different reviews (Logozzo et al., 2013; Reich et al., 2013; Zimmermann et al., 2015) (Table 1-1).

Table 1-1: Intraoral scanners available on the market

Name of IOS	**Manufacturer**	**City, Country**
3D Progress	MHT/ MHT Optic Research	Verona, Italy/ Niederhasli, Switzerland
AADVA	GC	Leuven, Belgium
Apollo DI	Sirona Dental Systems	Bensheim, Germany
Bluescan-I	A TRON3D	Klagenfurt, Austria
CEREC AC Bluecam	Sirona Dental Systems	Bensheim, Germany
CEREC AC Omnicam	Sirona Dental Systems	Bensheim, Germany
Condor	MFI	Gent, Belgium
CS 3500	Carestream	Rochester, USA
DigImprint	Steinbichler Optotechnik	Neubeuern, Germany
DirectScan	HINT – ELS	Griesheim, Germany
DPI-3D	DIMENSIONAL PHOTONICS INTERNATIONAL	Wilmington, USA
Dwio	Dental Wings	Montreal, Canada
E4D	D4D TECHNOLOGIES	Texas, USA
Intrascan	Zfx	Dachau, Germany
IOS FastScan	IOS TECHNOLOGIES	San Diego, USA
iTero	CADENT	Carlstadt, USA
iTero Element	Align Technology	San Jose, USA
KaVo Lythos	KaVo	Bilberach/Riss, Germany
Lava C.O.S.	3M ESPE	St. Paul, USA
True Definition Scanner	3M ESPE	St. Paul, USA
MIA3D	Densys 3D	Migdal Ha’Emek, Israel
Ormco Lythos	Ormco	Orange, USA
Planscan	Planmeca	Helsinki, Finland
Rainbow iOS	Dentium	Su-won, Korea
Trios Standard/Color	3SHAPE	Copenhagen, Denmark

Regardless of the quantity, only a few IOSs were tested in scientific and clinical studies. The most frequently applied intraoral scanners found in the literature were Lava C.O.S., iTero, Trios, and CEREC AC Bluecam or Omnicam. All of these are based on the three different major scanning technologies: active wavefront sampling technology, parallel confocal laser scanning microscopy, and active triangulation.

1. Active wavefront sampling technology (Lava C.O.S.) is a three-dimensional imaging system based on the rotating aperture principle with a structured blue light projection (Logozzo et al., 2013). The so-called 3D-in-motion video is recorded by the high definition video cameras, which capture the object from the different perspectives (Reich et al., 2013). Such an operating principle allows calculation of the three-dimensional coordinates in space, finding the spatial distances and creating the digital objects in real time (Kravitz, Groth, Jones, Graham, & Redmond, 2014). Usually, it requires a very light dusting with a scanning powder to reduce light reflection and, more importantly, to enhance the connection between captured images in the scanning process (Patzelt, Emmanouilidi, et al., 2014).

2. Parallel confocal laser scanning microscopy (iTero, Trios) is an optical technique to attain images from selected depths. The parallel laser beams are emitted from the camera, then reflected from the target surface and returned to the same optical path (Reich et al., 2013). Only the focused light can return and reach the processing sensor, whereas the out-of-focus light is removed (Kravitz et al., 2014). The complete 3D object is created by the “point-and-stitch” process, which, however, is slower than in the active wavefront sampling technology (Kravitz et al., 2014). On the other hand, the parallel confocal technique allows capturing the images in color and without scanning powder application. For this reason, the color wheel is required in the IOS of iTero (Logozzo et al., 2013). The biggest drawbacks of the color wheel are limited wavelength selection, vibration, and potential image shift (Wachman, Niu, & Farkas, 1997).
   The different versions of Trios IOS can perform either color or black and white scanning images. The color version allows better identification of the scanning details. Furthermore, there is an important possibility in implant prosthetics to scan the gingival profile before the non-individual scanbody is attached and the area is collapsed (Reich et al., 2013). In this way, the implant position is transferred with the help of the scanbody without damaging the

original emergence profile, which was already saved and could be added to the whole scan (Reich et al., 2013).

3. The active triangulation technique (CEREC AC Bluecam/Omnicam) is a non-contact digital data acquisition method. The main operating principle is that the light source emits either monochromatic light (CEREC AC Bluecam) or light with different wavelengths (CEREC AC Omnicam), which reflects from the target and is recorded by the equipment (Reich et al., 2013). Furthermore, distance information is obtained by the angle measurements of a triangular plane (Patzelt, Emmanouilidi, et al., 2014). Consequently, the separate images are also stitched and overlapped.

   The CEREC AC Bluecam IOS requires powder coating and performs colorless scans. On the contrary, CEREC AC Omnicam IOS does not require any powder application and performs true color scans.

1.3.1 Computer-aided impression making of the teeth

Most of the studies in the dental literature analyzing the capacity and at the same time indications of the different intraoral scanners were performed on one or more teeth and focused on restorative dentistry.

It was proved that the computer-aided impression-making approach could be a viable alternative to the conventional workflow for a single tooth restoration or 4-unit bridge (Guth, Keul, Stimmelmayr, Beuer, & Edelhoff, 2013; S. Y. Kim et al., 2014; Seelbach, Brueckel, & Wostmann, 2013). Another *in vivo* study (Boeddinghaus, Breloer, Rehmann, & Wostmann, 2015) was also consistent with this conclusion and stated that an intraoral digitation for a single-tooth restoration is an acceptable option for impression making procedure.

Additional studies compared both impression-making approaches on full dental arch study models. Specifically, both methods were applied to a full arch model with three prepared teeth in several *in vitro* studies (Ender & Mehl, 2011, 2015). It was concluded that an intraoral scan could be as accurate as conventional impressions. However, it was also stated that the digital impression shows higher local deviations at the distal part of the dental arch. The same authors, in another study (Ender & Mehl, 2013a), found that the digital approach generated less accurate results of trueness (58.6 ± 15.8 µm) and precision (32.4 ± 9.6 µm) in comparison with conventional impression with vinyl siloxanether material (trueness 20.4 ± 2.2 µm; precision 12.5 ± 2.5 µm).

Recently, the accuracy of four different intraoral scanners were compared on a full arch study model with all prepared teeth (Patzelt, Emmanouilidi, et al., 2014). The mean trueness values were found to be between 38 and 332.9 µm. The authors concluded that, despite comparable values of all tested intraoral scanners, the obtained inaccuracies might negatively influence the accuracy of the final restoration.

1.3.2 Computer-aided impression making for dental implants

Despite the new potential for digitization of dental implants brought about by developments of different IOSs, little is known about the accuracy of the digital approach on dental implants.

In order to make computer-aided implant impression and transfer three-dimensional implant positions into the digital system, the scanning abutments, i.e. so-called scanbodies, are required (Andriessen, Rijkens, van der Meer, & Wismeijer, 2014). These scanning elements have different geometrical properties, such as notches and emersions, which provide information about the implant position in three aspects: rotation, angle, and depth. The scanbodies are either metal-based or manufactured from polyether ether ketone (PEEK).

In 2004, a new implant impression-making technology appeared on the market that offered an alternative to the classical digital impression-making workflow of the dental implants. The so-called Robocast technology with the BellaTek Encode impression system, invented by Biomet 3i (Florida, USA), requires a two-piece healing abutment, which is occlusally coded, and either a digital or conventional abutment-level impression with an elastomer material. The occlusal code is transferred to the impression and recognized by the system.

If digital impression was performed, the system virtually designs and later fabricates the individual implant abutment. Afterwards, the abutment has to be tried in the mouth and intraorally digitized once again for the fabrication of the definitive restoration.

If conventional impression was performed and a stone cast was manufactured, the system recognizes the abutment code on the cast, designs the individual implant abutment virtually and positions the implant analog in the gypsum cast. Hereafter, the definitive restorations can be manufactured.

The potential advantages of the aforementioned workflows include a simplified implant impression-making technique and reduced chair time. Theoretically, the healing abutment is disconnected only once for insertion of the final restoration, which is also advantageous, because the peri-implant mucosal surface is not repeatedly traumatized.

Nevertheless, there is not much scientific information about the accuracy of the current system and only a few studies are available. In the *in vitro* study (Howell, McGlumphy, Drago, & Knapik, 2013), two parallel and two angled implants of 15° were placed in a dentate mandible with a Kennedy Class I defect. Conventional open-tray, closed-tray impressions and impressions with the Encode healing abutments were performed with a polyvinyl siloxane elastomeric material. The results showed that the Encode impressions/casts, together with the Robocast technology, were the least accurate approach in all categories. Namely, the Encode impressions were less accurate than the open-tray impressions of the nonparallel implants, and less accurate than both open- and closed-tray impressions of the parallel implants. It was also found that the Encode impressions of parallel implants were significantly more accurate than of nonparallel implants.

Some potential sources of error were suggested: supposedly, the technology-related issues, adhesively fixed implant analogs, accuracy of the impression material, and the height and proximity of the Encode abutment all might have influenced the accuracy of the definitive implant position.

Another study (Eliasson & Ortorp, 2012) was also in agreement with the above-mentioned conclusions. They placed six implants in the edentulous jaw in the region of canines and premolars. Three pick-up copings were positioned on one side and three Encode healing abutments on the other. The impressions were made with a vinylpolysiloxane material. Both techniques showed a certain displacement of the implant analogs: the pick-up technique gave a three-dimensional displacement of 31.2 µm, mean angle error of 0.14°, and mean rotation of the hexagon of 1.82°; the Encode abutments technique created a three-dimensional displacement of 79.5 µm, mean angle error of 0.41° and mean rotation of the hexagon of 2.88°. Nevertheless, it was concluded that, even though the difference in accuracy of both implant impression techniques was small, the Encode abutments and Robocast technology were less accurate.

Controversial data is present in the literature regarding the classical implant scanning approach as well.

3-unit bridges on two dental implants were fabricated in an *in vitro* study using conventional and computer-aided impression-making approaches (Karl, Graef, Schubinski, & Taylor, 2012). No significant difference was found between the CAD/CAM and conventionally fabricated frameworks. In conclusion, the authors stated that the accuracy of the digital approach seems to be as good as the conventional workflow.

Another study compared gypsum casts fabricated after the conventional impression-making procedure and milled casts manufactured after computer-aided impression making with an intraoral scanner (S. J. Lee, Betensky, Gianneschi, & Gallucci, 2014). The customized maxillary study model involved teeth and one implant in the left second premolar region. The results showed no

difference between the accuracy of conventionally and digitally manufactured models, except in the areas of the fossae and in the vertical implant position. The gypsum better represented the latter anatomical areas; however, both approaches significantly differed from the study model regarding the vertical implant position. The study concluded that the two model fabrication methods have similar accuracies.
The *in vitro* study (Papaspyridakos et al., 2015) was also in agreement with both of the previously discussed studies. The accuracy of the conventional and digital multiple implant impressions in the edentulous jaw was compared and, in conclusion, no statistically significant differences between the two approaches were found.

However, not all studies resulted in such favorable comparisons. The accuracy of conventional and computer-aided impression-making procedures was tested on differently angled implants (Lin, Harris, et al., 2015). The study model involved teeth and two implants. The two approaches were compared after gypsum and milled polyurethane models were fabricated. The results showed that the digital approach was less accurate than the conventional one. It was suggested to use an implant verification device to control the implant position when using the digital approach.
Another *in vivo* study (Andriessen et al., 2014) also showed adverse results. Two mandibular implants were scanned intraorally in the edentulous jaw. At the same time, conventionally manufactured gypsum casts were digitized extraorally. The accuracy of the intraoral impression-making approach was unacceptable, because the generated mean errors in distance and angle were 226 µm and - 2.582°, respectively.

1.3.3 The strategy of the scanning process

There is a lack of information in the literature about the accuracy of different scanning modalities. “Manufacturer’s recommendation” is the usual argument regarding the chosen scanning method mentioned in different studies (Andriessen et al., 2014; Gimenez et al., 2013; Karl et al., 2012; Papaspyridakos et al., 2015; Patzelt, Bishti, Stampf, & Att, 2014; Patzelt, Emmanouilidi, et al., 2014; Patzelt, Lamprinos, Stampf, & Att, 2014; van der Meer, Andriessen, Wismeijer, & Ren, 2012). To our knowledge, there is the only one *in vitro* study analyzing the accuracy of different scanning strategies (Ender & Mehl, 2013b). The authors used three IOSs (Lava C.O.S., COS; Cerec Bluecam, BC; iTero, CiT) and six scanning strategies: COS-straight (camera is straight and moves first occlusally, then orally, then buccally), COS-cross (camera moves from side to side along the dental arch in a so-called “zig-zag” fashion (Patzelt, Bishti, et al., 2014; Patzelt et al., 2013; van der Meer et al., 2012)), BC-top (optical impression only from an occlusal view), BC-diag (camera is angled by 30˚ and moves buccally and orally), BC-rot (the same strategy as BC-diag, but it starts occlusally and then moves bucally-orally with 30˚ angle), CiT (optical impression of dental arch buccally-orally and additional capturing of each preparation at a different angle). The trueness of COS-straight was 45.8 µm, COS-cross 90.2 µm, BC-top 52.5, BC-diag 29.4 µm, BC-rot 23.3 µm, CiT 35 µm. The study concluded that the selection of scanning strategy has an important influence on full-arch scanning accuracy, which also depends on the correct scanning protocol.

1.4 Preferences for conventional versus computer-aided approach

Several studies are present in the literature regarding patient preferences and time efficiency for computer-aided and conventional impression-making procedures.

Fifteen fully dentate patients were included in the *in vivo* study (Grunheid, McCarthy, & Larson, 2014) and thirty impressions were performed: 15 with an intraoral scanner and 15 with alginate impression material. 73.3% of the patients preferred the alginate impressions while 26.7% preferred the intraoral scanning procedure. The authors concluded that the conventional impression-making approach is still preferable in orthodontic treatment, because it takes less time and is better tolerated by the patients.

Patients' preferences were also analyzed in the clinical study (Wismeijer, Mans, van Genuchten, & Reijers, 2014). One implant was placed in the non-esthetic zone and either a digital or conventional (with polyether material) implant impression was made. The outcomes showed a significant preference for the intraoral scan procedure, mainly because of the unpleasant taste of the conventional impression material and preparatory activities. However, the digital impression in this study required more time to perform, which was negatively perceived by the patients.

On the contrary, a pilot study showed that the digital implant impression needs less time and is more easily performed by an inexperienced operator (S. J. Lee & Gallucci, 2013). The operators' preference likewise favored the IOS, because it requires less experience than the conventional procedure, and the additional re-scans have the potential to correct the entire impression without the need to repeat the whole procedure.

A recent *in vivo* study (Schepke, Meijer, Kerdijk, & Cune, 2015) dealt with operating time and patient compliance for an impression of a single implant in a complete dental arch. It was found that the digital impression procedure takes significantly less time (6 min 39 s) than the conventional one (12 min 13 s). Moreover, the patients reported a strong preference for the digital approach, because they felt less fear and were more comfortable with the convenience of the intraoral impression-making procedure.

Time efficiency of different intraoral scanners was analyzed in an *in vitro* study (Patzelt, Lamprinos, et al., 2014). The results were compared between conventional and computer-aided impression making approaches and showed that the digital approach was significantly faster than the conventional one. For instance, the digital impression of a single tooth abutment was up to 23 minutes faster; of two abutments, up to 22 minutes faster; and of the full dental arch with 14 abutments, up to 13 minutes faster. In conclusion, the authors stated that computer-aided impression making is beneficial for a more time-efficient workflow.

In the last years, the application of the computer-aided impression making procedures tended to be preferable. However, there is still not enough scientific data about the accuracy of the digital impression-making technologies in comparison to the conventional ones, especially regarding multiple implant digitation.

2 Aim of the study

The aim of the present study is to evaluate the accuracy of implant impressions in terms of distance and angle using computer-aided impression-making technology and conventional approaches in a standardized setting *in vitro*. It also aimed to verify the effect of implant angulation on the accuracy of digital and conventional impression making by means of trueness measurements.

The null hypothesis is that no significant difference in accuracy is present, neither among all implant analogs, nor between straight and tilted implant analogs. The comparison was conducted between computer-aided and conventional impression-making approaches with an intraoral scanner, polyether, and vinyl polysiloxane materials.

3 Outline of the study

The collected data of the digital and conventional impressions were analyzed in terms of trueness which is the comparison between the reference and the test datasets (DIN Deutsches Institut für Normung, 1997) (Figure 3-1).

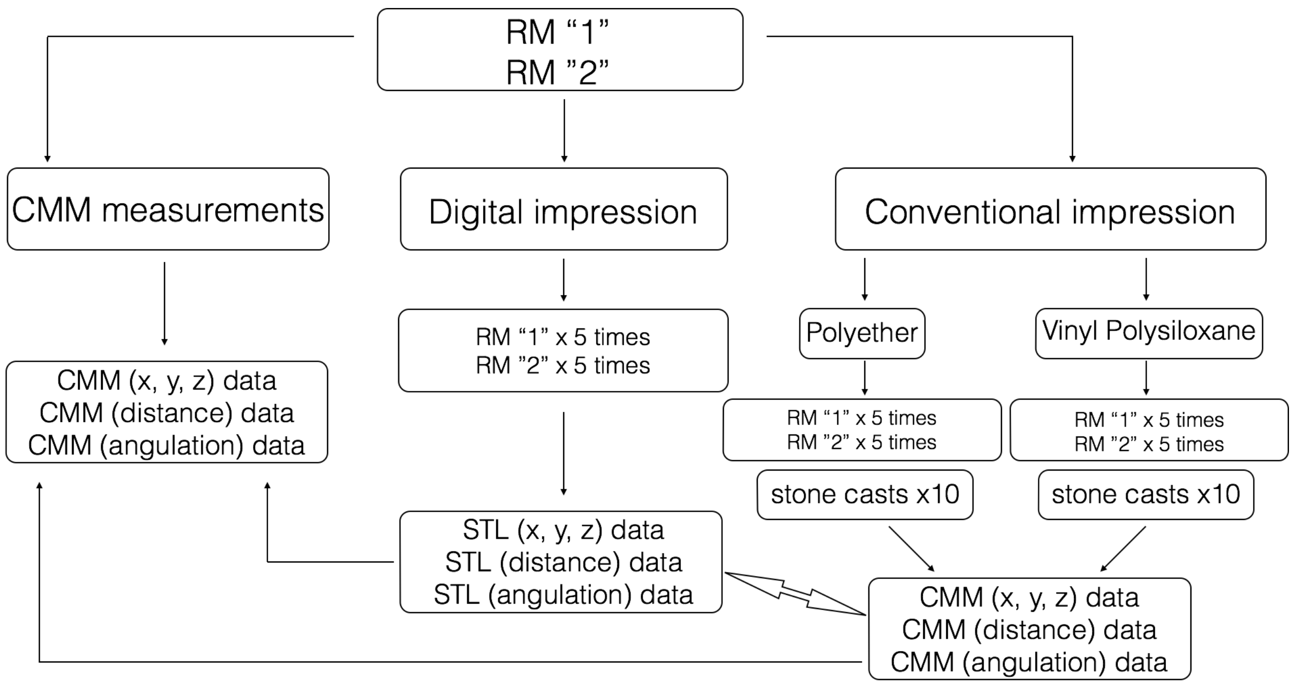

Figure 3-1: The scheme represents the workflow of the investigation.

First, both reference models (RM 1 and RM 2) were digitized with an industrial coordinate measuring machine (CMM) and the reference datasets were obtained (n=2). Secondly, each RM was scanned with the intraoral scanner five times (n=10). Afterwards, five conventional impressions with polyether material and five with vinyl polysiloxane material were performed by each RM (n=20). Stone casts were then manufactured (n=20) and digitized with the industrial scanner. Finally, the reference and test datasets were compared and evaluated.

4 Materials and Methods

4.1 Materials

4.1.1 Reference Model

A model of an edentulous mandible (Kavo Basic study model, Kavo Dental GmbH, Bilberach, Germany) was duplicated with a silicon material (picodent twinsil® 22, Picodent, Wipperfürth, Germany) to fabricate two study models. At first, these two duplicated reference models were poured with a polyurethane material (Alpa-Pur®, Shore A70, CHT BEZEMA R. Beitlich GMbH; Tübingen; Germany). In total, eight implants (Osseotite® 2 Certain® Implants, BIOMET, Inc., Warsawa, IN, USA) were placed following the implant placement protocol of the manufacturer. All implants had diameters (D) of 4 mm and lengths of 10 mm. Two different scenarios were created:

- Model 1: Four straight implants were placed interforaminally in the former area of the second incisors and the first premolars.
- Model 2: Two straight implants were placed interforaminally in the former area of the second incisors and two tilted lateral implants were placed in the former region of the first premolars with an angulation of 40-45˚.

All implants were covered with scannable abutments or so-called cover screws (4.1 mm (D) x 8 mm; Createch Medical®, Mendaro, Spain) and two silicon-replicating forms were produced. The cover screws were removed from each model, connected to the implant analogs (Certain® Implant Lab Analog, 4.1 mm (D), Biomet 3i, FL, USA) and positioned exactly in the same place of every replica form. The forms, including the fixed implant analogs, were poured with a polymethylmethacrylate material (ProBase Cold, Ivoclar Vivadent, Schaan/Liechtenstein) and polymerized in a pressure pot at 40 °C, 4 bar for 15 minutes (Figure 4-1). Thus, two reference models were fabricated. The reference models were stored in a cool, dark, well-ventilated room with a temperature of 21 ± 1 °C, relative humidity of 55 ± 3% and air pressure of 761 ± 5 mmHg.

a **b**

Figure 4-1 a, b: The reference models: a) Model 1 with four parallel implants, b) Model 2 with two parallel and two laterally tilted implants.

4.1.2 Reference Scanner

An industrial coordinate measuring machine (CMM) (Createch Medical S.L., Mendaro, Spain) situated in an independent laboratory was used to measure the three-dimensional (3D) position of each implant analog in the reference models and the test stone casts. Well-packed reference models were shipped to this laboratory one month after their production.

4.1.3 Intraoral Scanner (IOS)

The computer-aided impression (CAI) was taken with the 3M™ True Definition Scanner (software version 4.0.3.1, 3M ESPE, St. Paul, MN, USA). The True Definition Scanner is based on wavefront sampling technology. The scanning wand has three optical lenses, six light emitting diodes (LEDs) and one complementary metal oxide semiconductor (CMOS) sensor. LEDs are two-lead semiconductor light sources. The CMOS sensor is a digital image-capturing sensor, which converts the light into electronic signals. Each lens captures 20 images per second (20 Hz). The three images taken in parallel are matched together in real-time to create the three-dimensional digital object. The True Definition Scanner provides simultaneous image capturing, which is based on "3D-in-motion" video technology and generates 10.000 data points per image. The system requires scannable abutments, i.e. scanbodies, and a scanning powder, which prevents the effect of reflection and functions as a connector in the image overlapping process (Figure 4-2). The high-precision scanbodies used in the present investigation were manufactured from polyether ether ketone

(PEEK) (Createch Medical® 4.1 mm (D) x 8 mm (height), Mendaro, Spain). The applied high-resolution 3M™ scanning spray (3M ESPE, St. Paul, MN, USA) consists of titanium dioxide 50-60%, zirconium oxide 30-40%, and zinc stearate 5-10%. The size of the scanning powder particles is given as approximately 20 µm (manufacturer information).

a b

Figure 4-2 a, b: The reference models: Model 1 (a) and Model 2 (b) with scanbodies prepared for a computer-aided impression-making procedure.

4.1.4 Conventional Materials

For the conventional approach, two different impression materials were investigated:

- Polyether impression material (Impregum™ Penta™ Medium Body, 3M ESPE, St. Paul, MN, USA);
- Vinyl polysiloxane (VPS) impression material (Imprint™ 4 Penta™ Heavy and Regular, 3M ESPE, St. Paul, MN, USA).

Both materials are hydrophilic and applicable for implant impression making.

The impressions were taken using anatomically customized individual trays and conventional pick-up copings (4.1 mm (D) x 7.5 mm (H); Certain® EP® Pick-up Coping, Biomet 3i, FL, USA) (Figure 4-3). The individual trays provided 3 mm space relief for the impression material and the buccal-lingual stoppers. The stoppers ensured a stable tray position for each impression. The custom trays were made two weeks before taking the conventional impressions.

a

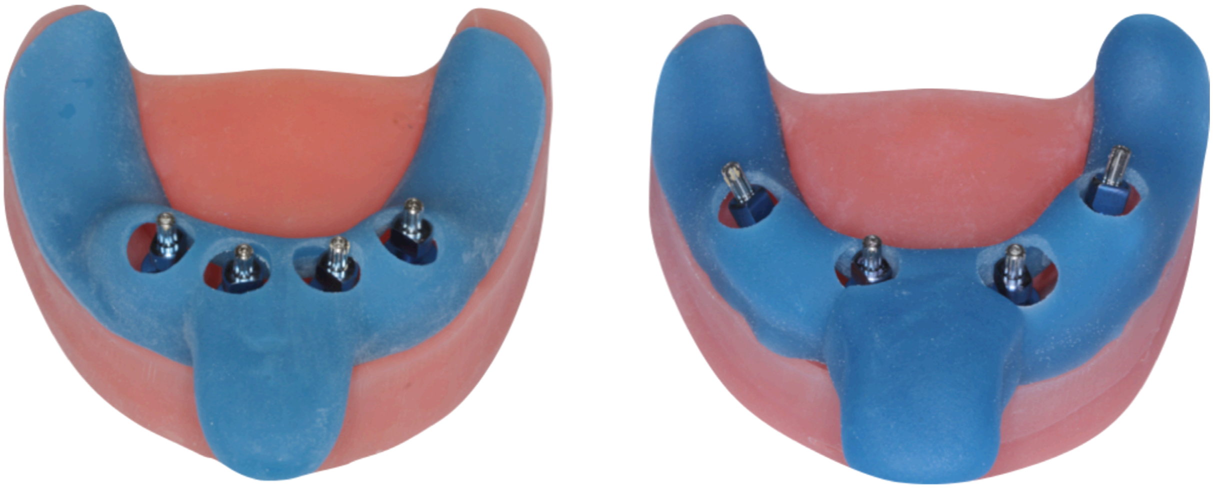

b

Figure 4-3 a, b: The reference models: a) Model 1 and 2 with pick-up copings; b) Model 1 and 2 with pick-up copings and individual trays for a conventional open tray impression making procedure.

The individual trays were manufactured from a light curing custom tray material (Megatray™, Megadenta Dentalprodukte GmbH, Radeberg, Germany) and afterwards two tray adhesive materials were used. 3M™ ESPE™ Polyether Tray Adhesive (St. Paul, MN, USA) was used for the polyether impression material and 3M™ ESPE™ VPS Tray Adhesive (St. Paul, MN, USA) for the VPS impression material.

To disinfect the impressions of both materials, a 2% solution consisting of didecyldimethylammonium chloride, glutaral and glyoxal (picodent® Tauchdesinfektion, Picodent, Wipperfürth, Germany) was used. The impressions were poured with a type 4 stone (crème brown color, pico-stone M®, Picodent®, Wipperfürth, Germany), which has an expansion of <0.1% (manufacturer information).

4.2 Methods

In order to obtain the reference data of the position of the 3D implant analogs, the CMM technique was used. Digital and conventional impression making methods were applied as the test methods and compared with reference data.

4.2.1 Measuring with CMM

CMM (Crista Apex, Mitutoyo, America Corporation, IL, USA) is a computer-controlled tactile measuring device with a certified accuracy by the National Entity of Accreditation (Geneva, Switzerland). The maximum permissible error for a length measurement is 1.9 + 3L/1000 µm according to the ISO 10360-2 - geometrical product specifications (ISO International organization for Standardization, 2009). It is calculated by using the mathematical formula:

$$E_x = [k + (\text{multiplier} * L) / 1000]\ \mu m$$

Where: E = the maximum measuring error, in microns, under the given conditions; k = systemic or inherent machine error that is not length dependent; multiplier – a constant that defines the travel-dependent error; and L = the length of travel over which the accuracy specification is desired, in millimeters (Optical Gaging Products Inc., 2015).

To define the measurements in space, i.e. in x-, y-, and z-axes, a ruby sphere with a diameter of 0.5 mm was used. Three different planes in the inner side of every implant analog neck and the connection plane on top were measured with a signal probe. The specific measuring approach was preceded in order to avoid the accumulation of measurement error. The measurement started from the zero position (the center point of the first implant analog located in the first premolar region of the fourth quadrant) to the point of interest (the center point of every further single implant analog) and came back to the zero position. The final position taken for each implant analog was the mean value of triplicate measurements.

The measurements with the CMM were applied for the reference models “1” and “2”, considering these data as the standard reference and control values. The conventional impression stone casts of both reference models were also measured with the CMM and compared to the standard reference.

4.2.2 Computer-aided impression making

The True Definition IOS was used to digitize both reference models in order to achieve digital datasets. All scans were made on the same day in the same room under the same aforementioned ambient conditions with a five-minute pause between each scan. The abovementioned scanbodies were hand-screwed on each implant analog and a light dusting with scanning powder was performed only once before starting the scanning process. The scanbodies were not removed until all scans were completed. According to the manufacturer's recommendations, a double gingival scanning method was applied: Following the specifications, the alveolar ridge was first scanned from the fourth to the third quadrant without capturing the scanbodies. After the scanning process was stopped and saved, the alveolar ridge was scanned once again from the third to the fourth quadrant and stopped again. To be able to continue the scanning process from one quadrant to the other, the wand was rotated clockwise (in the fourth quadrant) or counterclockwise (in the third quadrant) at the buccal area of the first premolars. The scanbodies were digitized separately in detail and the scan process was stopped after each of them. Finally, the data was saved and the prescription was filled. Special attention was given to the IOS wand position while scanning: it was aligned to the alveolar ridge parallel to the scanning surface and the needed focal distance was kept. Each reference model was scanned 5 times by one operator.

The operator was trained by the manufacturer in a two-day digital implant impression-making course. Approximately 30 scans were executed before the investigation began.

4.2.3 Conventional Impression

All conventional impressions were made within three days in the same room under the same aforementioned ambient conditions corresponding to the environment of the computer-aided impression making. Ten individual trays were laboratory-manufactured for an open tray implant impression technique. A thin layer of adhesive for either the polyether or VPS material was applied and allowed to dry for at least five minutes. After positioning the pick-up copings on the implant analogs of the reference models, the impression was made.

The polyether impression material - Impregum™ Penta™ Medium Body was used together with a monophase impression-making technique. First the syringe, then the tray were filled with the impression material. Following this sequence, primarily the material was applied around the pick-up copings, then, the loaded tray was positioned and secured without pressure until the setting was complete. After the setting time (6 min.), the impression was separated from the reference model. This procedure was repeated four times to obtain five impressions (Figure 4-4).

a **b**

Figure 4-4 a, b: The conventional impressions of both reference models performed with a polyether impression material. Reference Model 1 (a) and Model 2 (b) with and without fixed implant analogs.

The VPS material was used according to a double mix impression technique. While the tray was loaded with the heavy-bodied material, the regular material was applied around the pick-up copings. Then, the loaded tray was positioned and secured on the reference model. After four minutes, the impression was separated from the reference model. This procedure was repeated four times to obtain a total of five impressions (Figure 4-5).

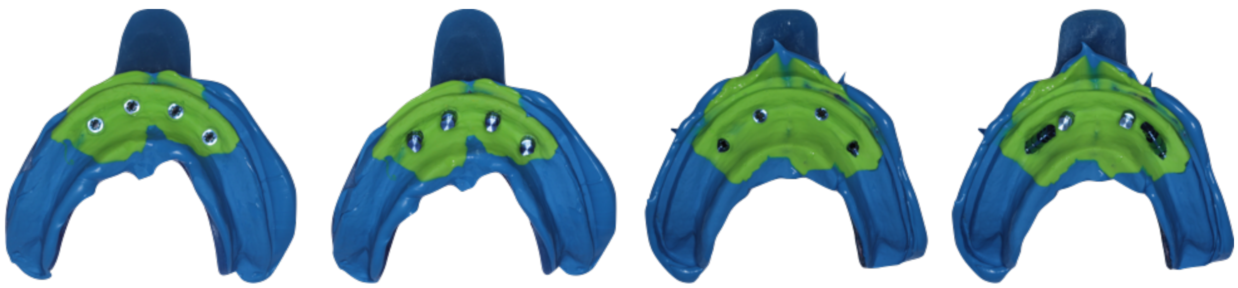

a **b**

Figure 4-5 a, b: The conventional impressions of both reference models performed with a vinyl polysiloxane impression material. Reference Model 1 (a) and Model 2 (b) with and without fixed implant analogs.

Each impression was placed into a disinfection solution for 10 minutes, then rinsed under running cold water for approximately 15 seconds. After 30 to 45 minutes, the impressions were poured with stone. To avoid bubbles in the cast, each impression was briefly pre-rinsed with cold water and dried with air before pouring. Gypsum powder (200 g) and 44 ml of distilled water were used to produce each cast. The vacuum mixing time was 40 s. 60 minutes later, the stone casts were separated from the impression material, slightly shaped with a trimmer device and stored in a cool, dark, well-ventilated room with a temperature of 21 ± 1°C, relative humidity of 55 ± 3% and air pressure of 761 ± 5 mmHg. After one week, well-packed stone casts were shipped to the Createch Medical laboratory for the CMM measurements (Figure 4-6).

a **b**

Figure 4-6 a, b: The stone casts of the reference Model 1 (a) and 2 (b) prepared after conventional impression making procedures.

4.2.4 Data Analysis

The information about the 3D implant analogs' (IA) positions was provided by coordinates (x, y, z). Two parameters were included into the analysis: distance (in mm) and angulation (in grades). Both aforementioned parameters, 3D IAs position of two reference models and 20 stone casts were provided by Createch Medical. Ten scans made with the True Definition IOS were retrieved into the Standard Tessellation Language (STL) format. The STL file and the original CAD file of the scanbody were matched using a best-fit algorithm, so that the corresponding digital implant analog would be adapted to the scanbody. In this way, the final STL file of the whole digital scan was prepared and analyzed using 3D evaluation software (Geomagic Qualify™ 2012, Geomagic, Morrisville, USA). The 3D analyses were performed after implant analogs and scanbodies were separated from the surrounding structures.

The differences between the datasets of the distances and angles in the reference models and digital/conventional impressions were calculated by subtraction. If the distance or angulation in the tested digital scan or conventional impression was bigger than in the reference model, the outcome was a positive value, if smaller it was a negative one.

4.2.4.1 Analysis of the inter-implant distance

The distance between two IAs was calculated as the distance between the center points of each IA. The center point itself was defined as the intersection between the IA rotational axis and the upper connection plane (Figure 4-7).

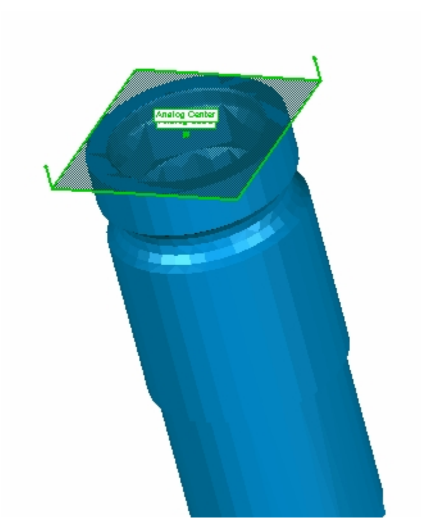

Figure 4-7: The 3D image demonstrates the center point of the implant analog.

For defining the center point with the use of cylinder-shaped scanbodies, it was assumed that the axis and the bottom plane of the scanbody correspond with the rotational axis and the upper plane of the IA (Figure 4-8).

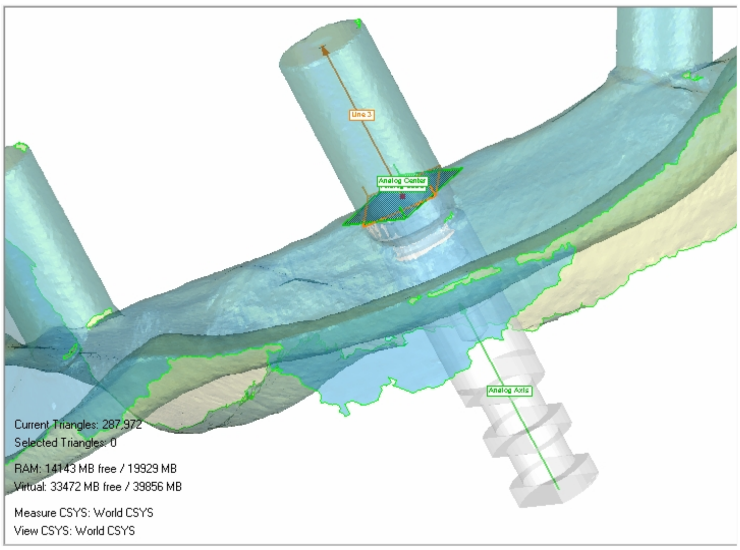

Figure 4-8: The 3D image defines the center point of the implant analog using a scanbody.

To be able to measure the 3D distance between two IAs, the IA located in the first premolar region of the fourth quadrant was always used as the starting point (Figure 4-9).

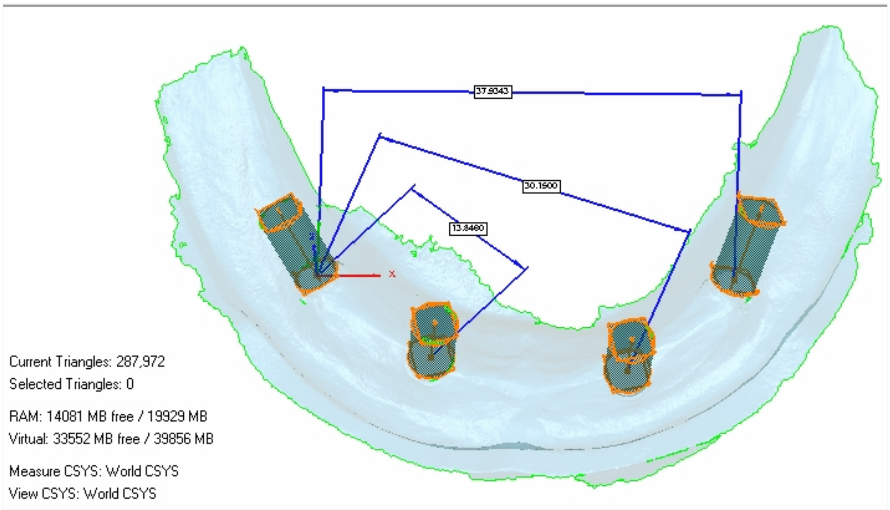

Figure 4-9: The 3D distances found between the center points of each implant analog.

Based on the mathematical formula: $d_{AB} = \sqrt{(x_A - x_B)^2 + (y_A - y_B)^2 + (z_A - z_B)^2}$, every 3D distance (d) between the center point A with the coordinates in the space (x_A, y_A, z_A) and the center point B with the coordinates (x_B, y_B, z_B) was calculated. The obtained results were compared to the reference data obtained from the CMM measurements and the difference was statistically evaluated.

4.2.4.2 Analysis of the inter-implant angulation

The angle of every IA was the defined as the angular difference found between the axes of each IA. The axis of the IA located in the first premolar region of the fourth quadrant was considered as the reference line. This reference line was copied and pasted on every other IA center point using the analysis software (Geomagic Qualify™) (Figure 4-10).

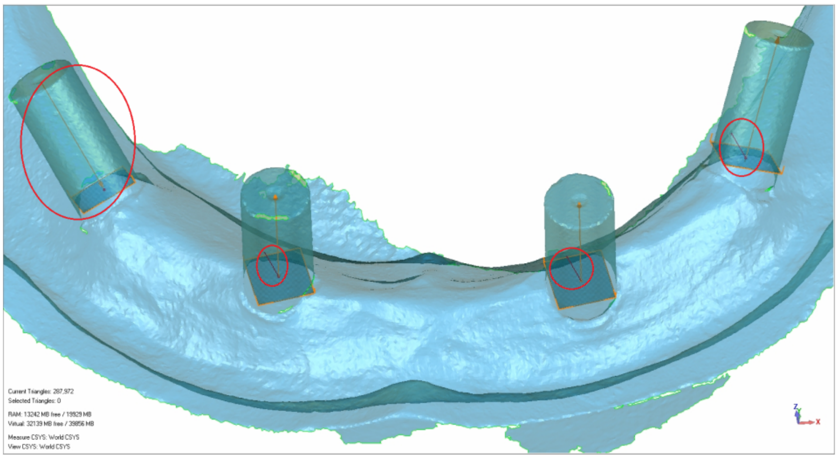

Figure 4-10: The reference axis of the first premolar in the fourth quadrant is chosen and transferred on every other implant analog.

Afterwards, the software provided the unitary vectors based on the mathematical formula: $\theta = \cos^{-1}\left(\frac{\vec{A}.\vec{B}}{|\vec{A}|.|\vec{B}|}\right)$

The angles were analytically calculated in radians. To be able to convert radians into grades, radian values were multiplied by 180 and divided by π (Figure 4-11). The angle of each IA was compared with the reference data (CMM measurements) and the difference was statistically evaluated.

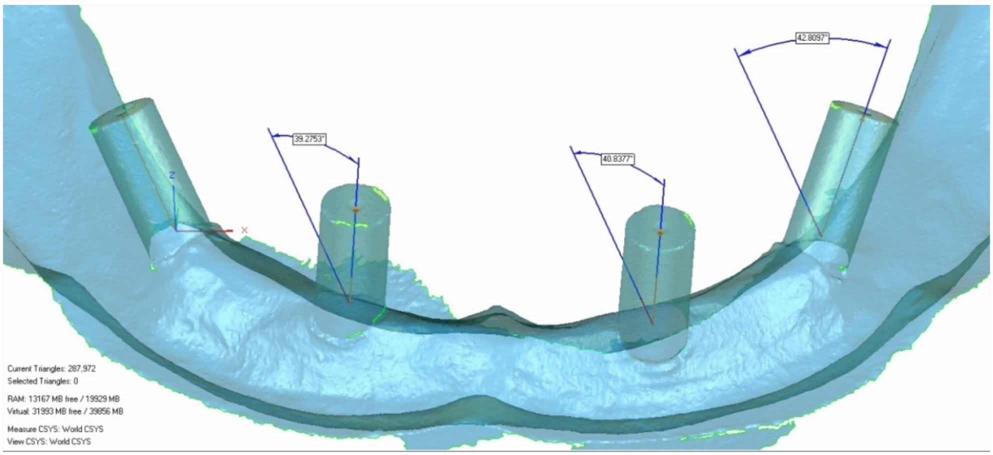

Figure 4-11: The 3D image shows the principle of finding the angle of every implant analog.

The axis of the implant analog, located in the first premolar region of the fourth quadrant, was pasted on all other analogs. In this way, the angle between the original analog axis and the pasted axis was found.

4.2.5 Statistical Analyses

Statistical analyses were performed to investigate discrepancies for accuracy of the distance and angle between the implant analogs in two reference models. The results were compared between the digital and conventional impression methods as well as between the two different conventional materials.

The statistical analyses were represented by the overall evaluation and with respect to each implant analog position. Different positions of implant analogs determined three different distances between them, i.e. the distance “1-2”, “1-3”, “1-4”. The relation between different implant analogs “1-2”, “1-3”, “1-4” was also evaluated in terms of angle. Additionally, a percentage expression evaluation of trueness was included for a better availability of comparison.

Medians, means and standard deviations (SD) were computed for a descriptive statistical analysis. Using a robust form of Levene’s test statistic for the equality of variances, mean was replaced with median (proposed by Brown and Forsythe) for each model.

One-way ANOVA was used to compare the differences of the group means. Boxplots were prepared for a graphical representation.

All calculations were performed with the statistical software STATA 13.1 (Stata Corp. LP, Texas, USA). The threshold of statistical significance was set to $p<0.05$.

5 Results

The reliability of the conventional and digital approach of the impression making was expressed in terms of trueness. The deviations in distances and angulations between the implant analogs occurred in positive and negative ranges. The ranges and their percentage expressions were compared. All values were represented by the mean and SD.

5.1 Distance deviation

5.1.1 Reference Model 1

The overall mean deviations for the IOS (n=15), Impregum (n=15), and Imprint (n=15) were 9.46 ± 16.04 µm, 12.22 ± 16.93 µm, and 12.74 ± 12.5 µm, respectively. The differences identified in variability (p=0.464) and in mean values between Impregum and IOS (p=0.533), Imprint and IOS (p=0.736), and Imprint and Impregum (p=0.905) were not statistically significant (Figure 5-1).

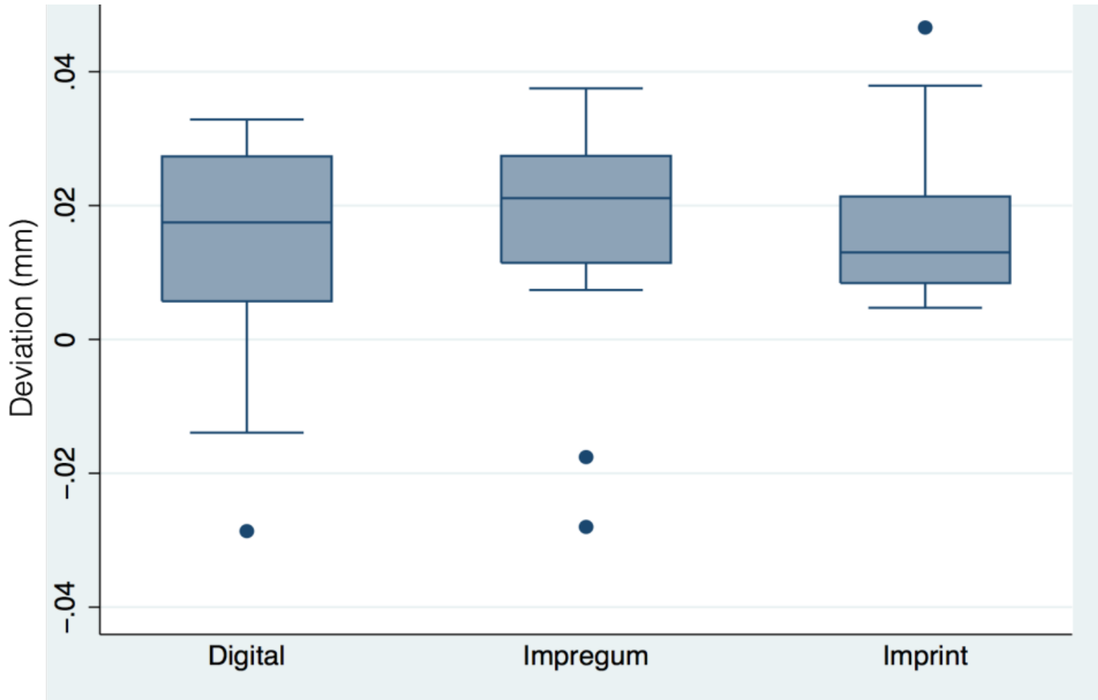

Figure 5-1: Boxplots representing the distance deviation of each impression-making group in the overall analysis.

The overall mean values for the IOS (n=15), Impregum (n=15), and Imprint (n=15) and expressed in percent were 0.1 ± 0.11%, 0.11 ± 0.11%, 0.1 ± 0.08%, respectively. No statistical significance in variability (p=0.216) or in mean values (Impregum vs. IOS p=0.739, Imprint vs. IOS p=0.987, Imprint vs. Impregum p=0.934) was found (Figure 5-2).

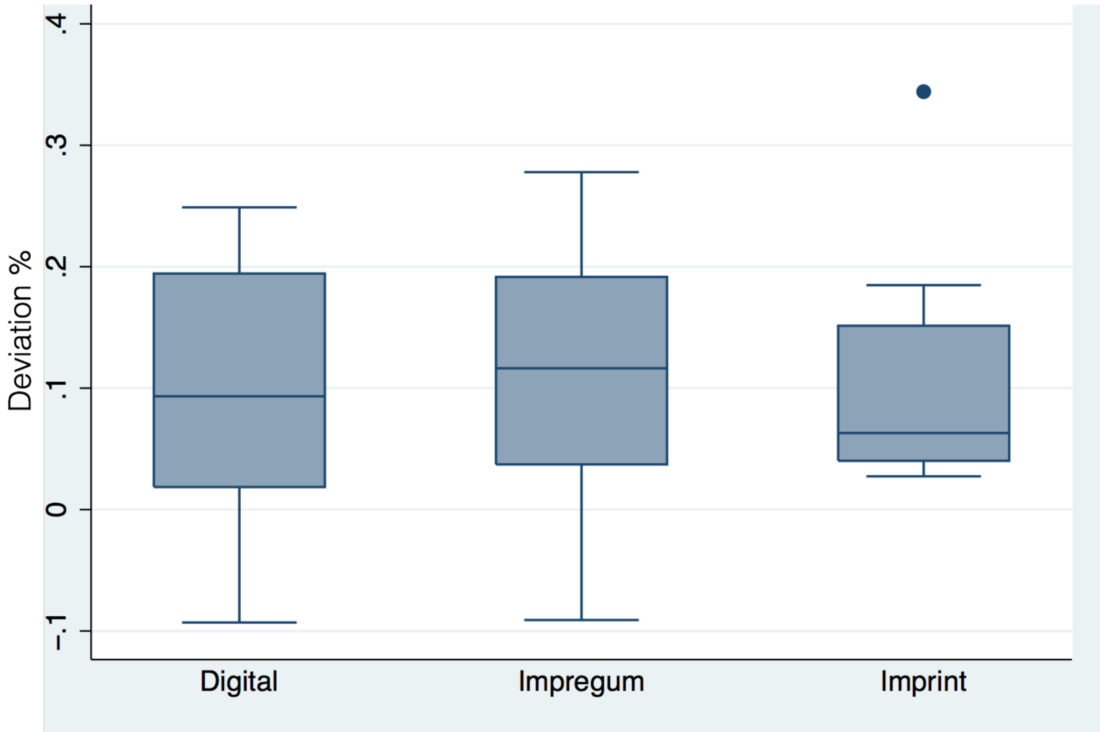

Figure 5-2: Boxplots representing the percentage expression of the distance deviation of each impression-making group in the overall analysis.

Separate distances between implant analogs “1-2”, “1-3”, “1-4” were analyzed according to each analog position. The statistical analyses of the distance discrepancies and the percentage expression showed no difference in variability and in mean values among all impression-making methods for all distances (Table 5-1, 5-2; Appendix: Figure 11-1, 11-2).

Table 5-1: Comparison of mean values in distance deviation of each analyzed distance

Impressioning Group	Distance	Difference in distance (µm)	p-value
Impregum vs. IOS	1-2	2.18	0.686
Imprint vs. IOS	1-2	-5.88	0.287
Imprint vs. Impregum	1-2	-8.06	0.313
Impregum vs. IOS	1-3	-7.89	0.605
Imprint vs. IOS	1-3	-7.54	0.369
Imprint vs. Impregum	1-3	0.35	0.966
Impregum vs. IOS	1-4	16.65	0.187
Imprint vs. IOS	1-4	26.45	0.107
Imprint vs. Impregum	1-4	9.8	0.426

Table 5-2: Comparison of variability and its percentage expression in the distance deviation of each analyzed distance

Material	Distance	Datasets	Mean (µm)	SD (µm)	Mean (%)	SD (%)	p-value
IOS	1-2	5	23.66	± 4.24	0.21	± 0.04	0.181
Impregum	1-2	5	25.84	± 4.76	0.23	± 0.04	
Imprint	1-2	5	17.78	± 12.97	0.16	± 0.12	
IOS	1-3	5	20.76	± 10.45	0.09	± 0.05	0.368
Impregum	1-3	5	12.88	± 18.75	0.06	± 0.09	
Imprint	1-3	5	13.23	± 5.39	0.06	± 0.02	
IOS	1-4	5	-6.5	± 15.88	-0.02	± 0.05	0.902
Impregum	1-4	5	10.16	± 23.72	0.03	± 0.08	
Imprint	1-4	5	19.95	± 15.67	0.06	± 0.05	

5.1.2 Reference Model 2

The overall mean values for the IOS (n=15), Impregum (n=15), and Imprint (n=15) were 35.78 ± 24.22 µm, 19.78 ± 21 µm and 4.87 ± 21.34 µm, respectively. The data analyses yielded statistically significant differences in mean values between Impregum and IOS (p=0.006), Imprint and IOS (p<0.0001), and Imprint and Impregum (p=0.010). Regarding variability, a statistically significant difference was found only between IOS and Imprint (p=0.035) (Figure 5-3).

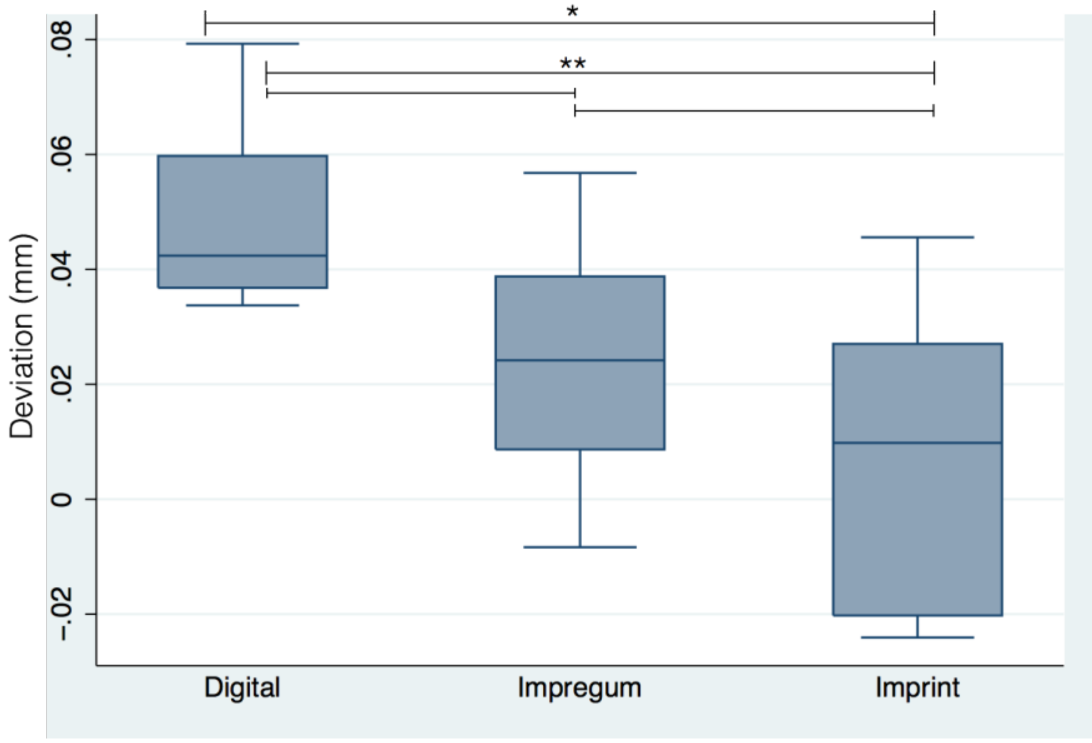

Figure 5-3: Boxplots representing the distance deviation of each impression-making group in the overall analysis. Asterisk: p<0.05 (in variability values), double asterisk: p<0.05 (in mean values).

The overall mean values performed with IOS (n=15), Impregum (n=15), and Imprint (n=15) and expressed in percent were 0.2 ± 0.07%, 0.08 ± 0.06%, and -0.00096 ± 0.1%, respectively. Statistically significant differences in mean values were found between Impregum vs. IOS (p<0.0001), Imprint vs. IOS (p<0.0001), Imprint vs. Impregum (p=0.006). However, all three impression-making groups did not significantly differ in variability (p=0.172) (Figure 5-4).

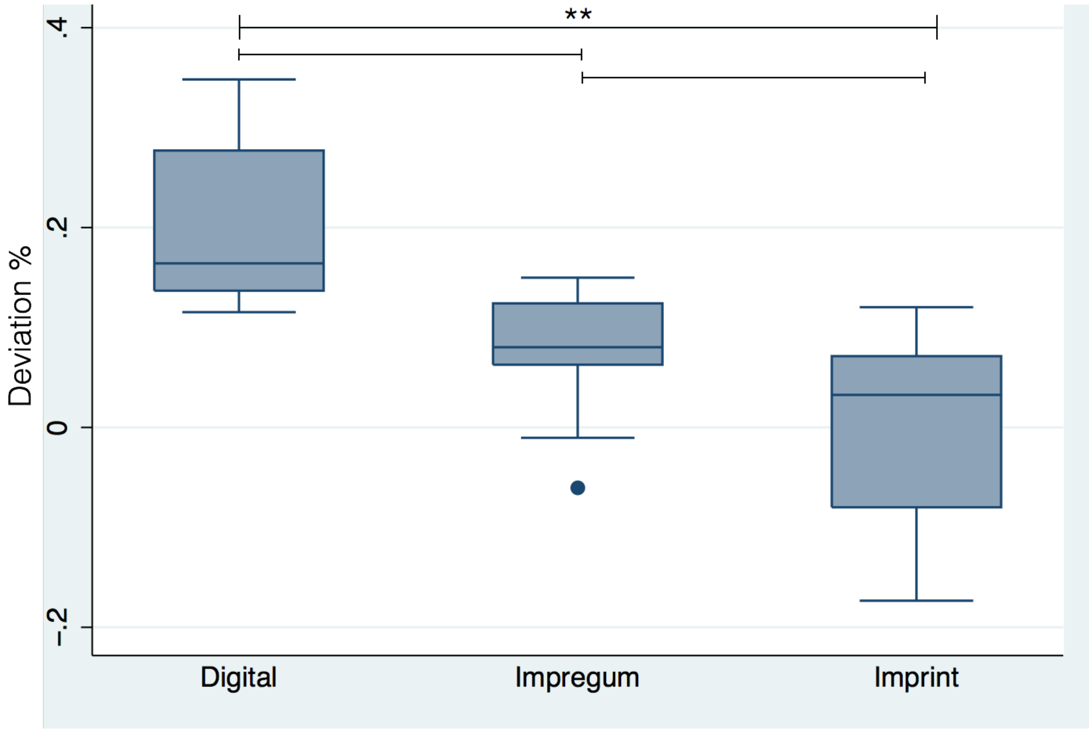

Figure 5-4: Boxplots representing the percentage expression of the distance deviation of each impression-making group in the overall analysis. Double asterisk: $p<0.05$ (in mean values).

The one-way ANOVA of the distance discrepancies and the percentage expression analyses (CI 95%, $p<0.05$) showed statistically significant mean differences between Imprint and IOS for all distances among implant analogs. In the Impregum and IOS groups, the significant mean differences were found only for the distances "1-2" and "1-4", and in the groups of Imprint and Impregum only for the distances "1-2" and "1-3". Nevertheless, there were no statistically significant differences found for variability among the three impression-making methods for all distances (Table 5-3, 5-4; Appendix: Figure 11-3, 11-4).

Table 5-3: Comparison of mean values in distance deviation of each analyzed distance

Impressioning Group	Distance	Difference in distance (µm)	p-value
Impregum vs. IOS	1-2	-35.11	< 0.0001
Imprint vs. IOS	1-2	-51.1	< 0.0001
Imprint vs. Impregum	1-2	-15.99	0.038
Impregum vs. IOS	1-3	-12.49	0.116
Imprint vs. IOS	1-3	-42.2	< 0.0001
Imprint vs. Impregum	1-3	-29.71	0.002
Impregum vs. IOS	1-4	-16.42	0.043
Imprint vs. IOS	1-4	-30.36	0.003
Imprint vs. Impregum	1-4	-13.94	0.079

Table 5-4: Comparison of variability and its percentage expression in the distance deviation of each analyzed distance

Material	Distance	Datasets	Mean (µm)	SD (µm)	Mean (%)	SD (%)	p-value
IOS	1-2	5	39.71	± 5.22	0.29	± 0.04	0.356
Impregum	1-2	5	4.59	± 9.77	0.03	± 0.07	
Imprint	1-2	5	-11.39	± 15.16	-0.08	± 0.11	
IOS	1-3	5	39.51	± 5.51	0.13	± 0.02	0.096
Impregum	1-3	5	27.02	± 6.05	0.09	± 0.02	
Imprint	1-3	5	-2.69	± 18.43	-0.01	± 0.06	
IOS	1-4	5	63.91	± 10.12	0.17	± 0.03	0.937
Impregum	1-4	5	47.49	± 12.66	0.13	± 0.03	
Imprint	1-4	5	33.55	± 11.53	0.09	± 0.03	

5.1.3 Reference Model 1 versus Model 2

The datasets of the reference model 1 (with four straight implants) and model 2 (with two straight and two tilted implants) were compared with regard to distance deviation in all three impression-making approaches. Statistically significant differences in overall variability between model 1 (15 datasets) and model 2 (15 datasets) were found in the group with Imprint (p=0.007). There was no significant difference for the IOS (p=0.543) or Impregum approaches (p=0.443). Nevertheless, the statistically significant difference was found in the group of Impregum in the percentage expression of variability (p=0.028). However, the difference in the overall mean values between both reference models was statistically significant only in the IOS group (p<0.0001). Furthermore, one-way ANOVA analysis of the percentage expressions showed significant differences in mean values in the group of Imprint (p=0.008) and IOS (p=0.007) (Figure 5-5, 5-6).

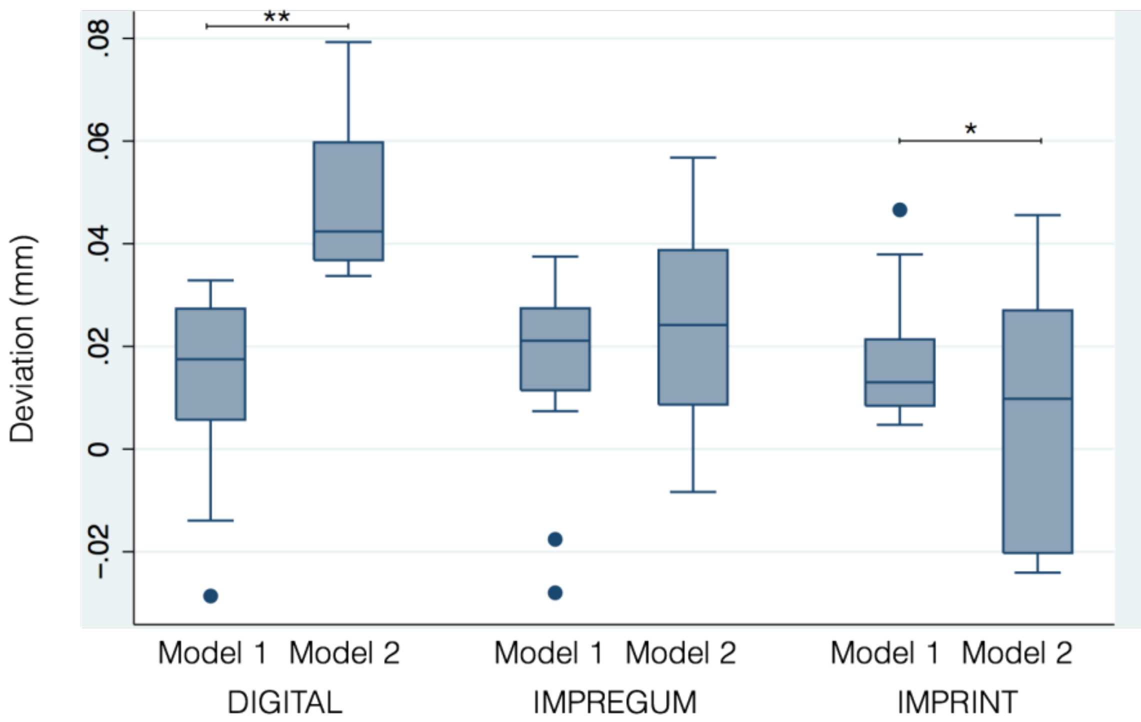

Figure 5-5: Boxplots representing the distance deviation in the reference model 1 and model 2 for all impression-making methods. Asterisk: p<0.05 (in variability values), double asterisk: p<0.05 (in mean values).

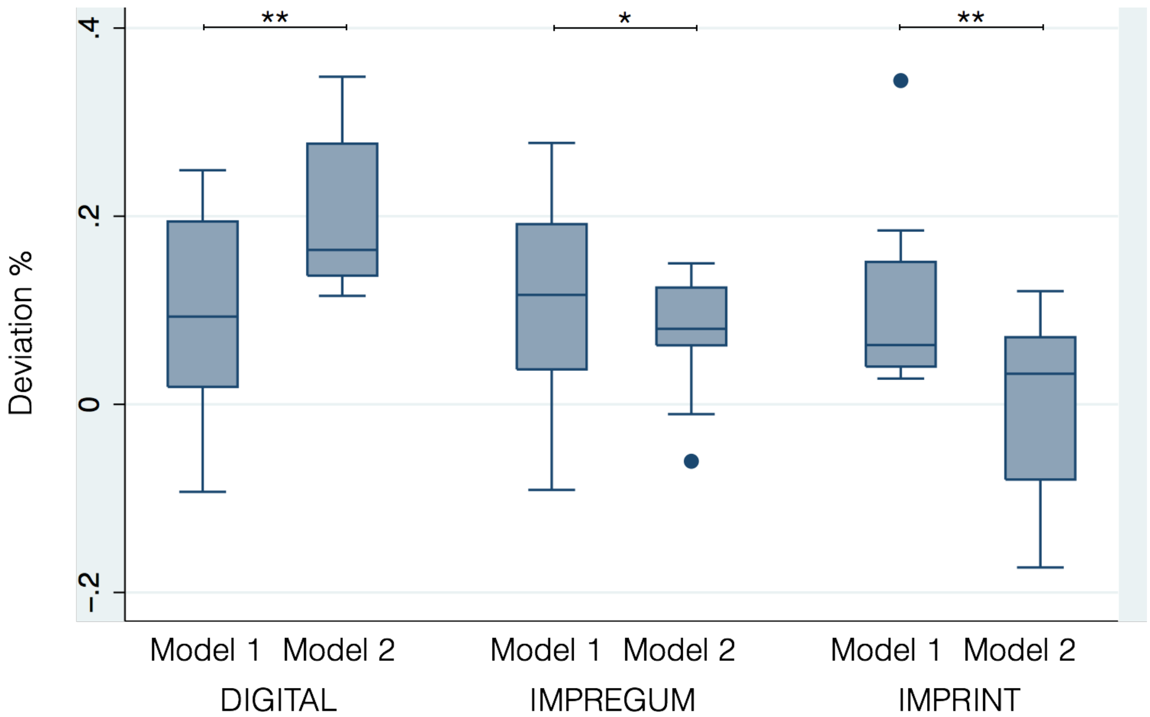

Figure 5-6: Boxplots representing the percentage expression of the distance deviation in all impression-making methods and both the reference models. Asterisk: $p<0.05$ (in variability values), double asterisk: $p<0.05$ (in mean values).

The statistical analysis of variability between the datasets of the reference model 1 and model 2, including all three impression-making methods, showed no statistically significant difference between the distances of the implant analogs. However, significant mean differences were found in all groups, except in the Impregum group for the distance "1-3" and in the Imprint group for the distances "1-3" and "1-4". The significant mean differences of the percentage expression were found in the IOS and Impregum groups for the distances "1-2" and "1-4", and in the Imprint group for the distances "1-2" and "1-3" (Table 5-5; Appendix: Figure 11-5 – 11-10).

Tab. 5-5: Comparison of variability and mean values in the distance deviation of each analyzed distance in both reference models

Material	Distance	p-value (variability)	p-value (variability %)	p-value (mean)	p-value (mean %)
IOS	1-2	0.992	0.728	0.001	0.017
Impregum	1-2	0.307	0.475	0.003	0.001
Imprint	1-2	0.76	0.981	0.011	0.01
IOS	1-3	0.176	0.069	0.008	0.152
Impregum	1-3	0.266	0.21	0.147	0.456
Imprint	1-3	0.089	0.141	0.101	0.047
IOS	1-4	0.337	0.207	< 0.0001	0.0001
Impregum	1-4	0.64	0.509	0.015	0.039
Imprint	1-4	0.854	0.687	0.157	0.397

5.2 Angle deviation

5.2.1 Reference Model 1

The overall mean values performed with IOS (n=15), Impregum (n=15), and Imprint (n=15) were 0.17 ± 0.14°, 0.07 ± 0.1°, and 0.08 ± 0.07°, respectively. The data analyses yielded statistically significant differences in mean values between Impregum and IOS (p=0.002), Imprint and IOS (p=0.003), but the differences in variability were not statistically significant among the three groups (p=0.728) (Figure 5-7).

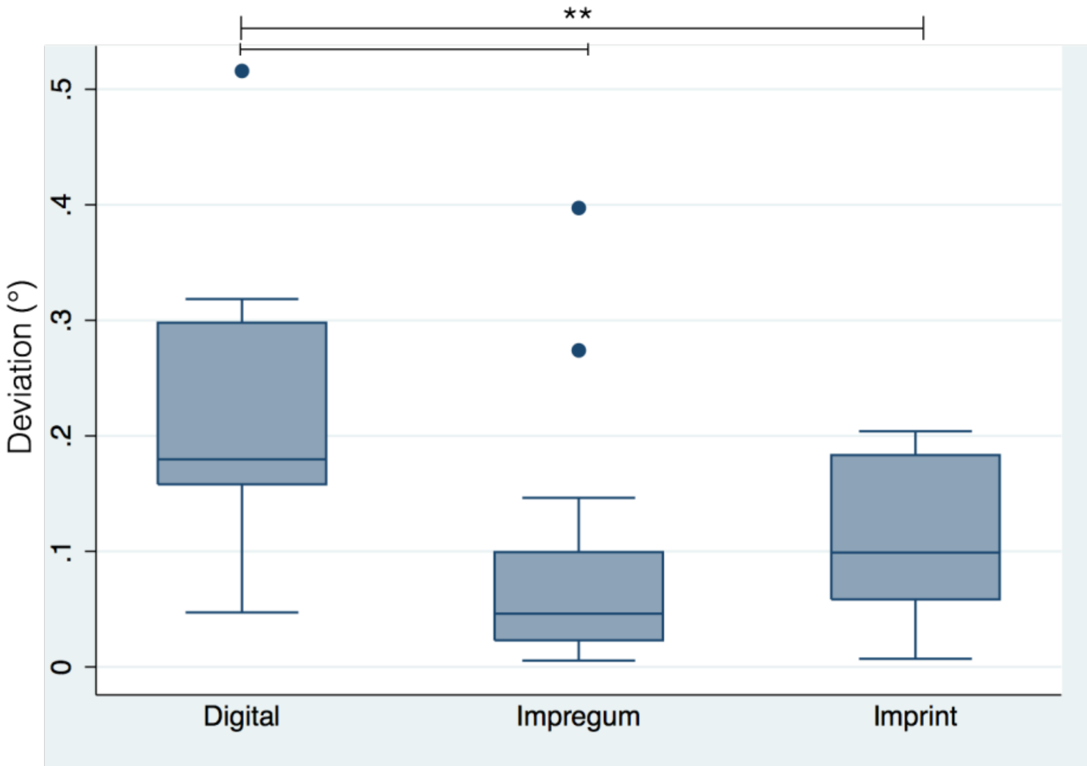

Figure 5-7: Boxplots representing the angle deviation of each impression-making group in the overall analysis. Double asterisk: p<0.05 (in mean values).

The overall mean deviation calculated from the reference with IOS (n=15), Impregum (n=15), and Imprint (n=15) and expressed in percent were 6.77 ± 2.78%, 2.69 ± 3%, 3.38 ± 1.87%, respectively. Statistically significant difference in mean was found between Impregum vs. IOS ($p<0.0001$) and Imprint vs. Digital (0.001). However, there was no significant difference found in variability ($p=0.808$) (Figure 5-8).

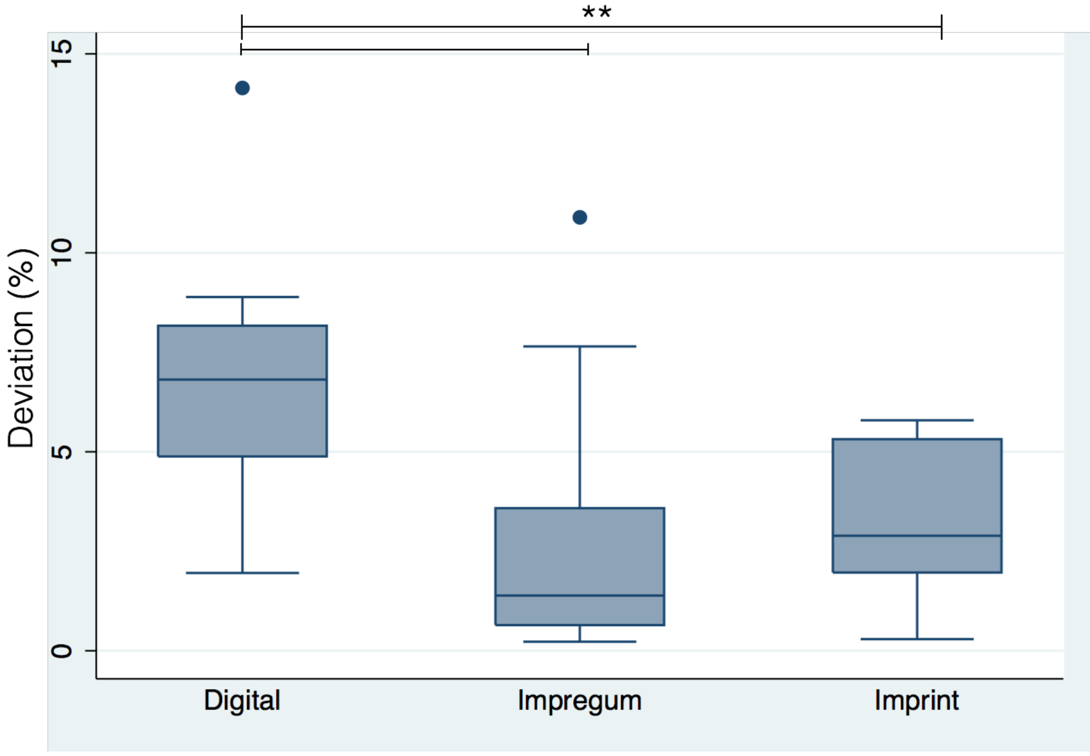

Figure 5-8: Boxplots representing the percentage expression of the deviation angle of each impression-making group in the overall analysis. Double asterisk: p<0.05 (in mean values).

The analyses according to each implant's analog position and the percentage expression showed a statistically significant difference in mean only between Impregum and IOS in the distances "1-2" and "1-4". There was no statistically significant difference found in variability between all impression making methods for all distances (Table 5-6, 5-7; Appendix: Figure 11-11, 11-12).

Table 5-6: Comparison of mean values in angle deviation of each analyzed distance

Impressioning Group	Distance	Difference in angle (˚)	p value
Impregum vs. IOS	1-2	-0.09	0.028
Imprint vs. IOS	1-2	-0.06	0.06
Imprint vs. Impregum	1-2	0.03	0.374
Impregum vs. IOS	1-3	-0.14	0.064
Imprint vs. IOS	1-3	-0.11	0.083
Imprint vs. Impregum	1-3	0.04	0.538
Impregum vs. IOS	1-4	-0.16	0.046
Imprint vs. IOS	1-4	-0.17	0.099
Imprint vs. Impregum	1-4	-0.004	0.96

˚ = degrees

Table 5-7: Comparison of variability and its percentage expression in the angle deviation of each analyzed distance

Material	Distance	Datasets	Mean (˚)	SD (˚)	Mean (%)	SD (%)	p-value
IOS	1-2	5	0.13	± 0.06	5.58	± 2.3	0.905
Impregum	1-2	5	0.04	± 0.04	1.75	± 1.59	
Imprint	1-2	5	0.07	± 0.05	2.94	± 2.1	
IOS	1-3	5	0.22	± 0.07	6.22	± 2.01	0.961
Impregum	1-3	5	0.08	± 0.11	2.28	± 3.01	
Imprint	1-3	5	0.12	± 0.08	3.27	± 2.31	
IOS	1-4	5	0.31	± 0.13	8.49	± 3.45	0.642
Impregum	1-4	5	0.15	± 0.15	4.05	± 4.04	
Imprint	1-4	5	0.14	± 0.05	3.95	± 1.34	

˚ = degrees

5.2.2 Reference Model 2

The overall mean values performed with IOS (n=15), Impregum (n=15) and Imprint (n=15) were 0.22 ± 0.19°, 0.04 ± 0.04°, and 0.16 ± 0.16°, respectively. The overall mean values expressed in percent were IOS 0.73 ± 0.38%, Impregum 0.14 ± 0.09%, and Imprint 0.53 ± 0.36%. The data analyses yielded statistically significant differences in both mean values and variability together with their percentage expression between Impregum and IOS, and Imprint and Impregum. However, there was no statistically significant difference found between Imprint and IOS (Table 5-8; Figure 5-9, 5-10).

Table 5-8: Comparison of variability and mean values in the overall analysis of the angle deviation

Material	Datasets	p-value (mean)	p-value (mean %)	p-value (variability)	p-value (variability %)
Impregum vs. IOS	30	< 0.0001	< 0.0001	0.0004	0.001
Imprint vs. Impregum	30	0.001	0.001	< 0.0001	0.0002
Imprint vs. IOS	30	0.078	0.079	0.968	0.961

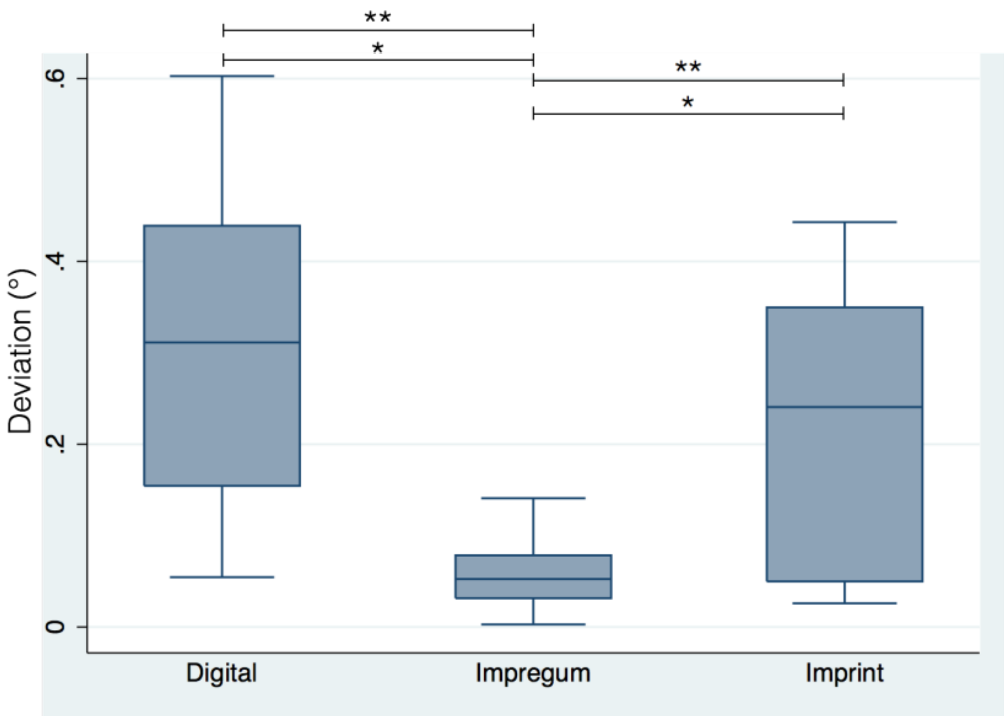

Figure 5-9: Boxplots representing the angular deviation of each impression-making group in the overall analysis. Asterisk: p<0.05 (in variability values); double asterisk: p<0.05 (in mean values).

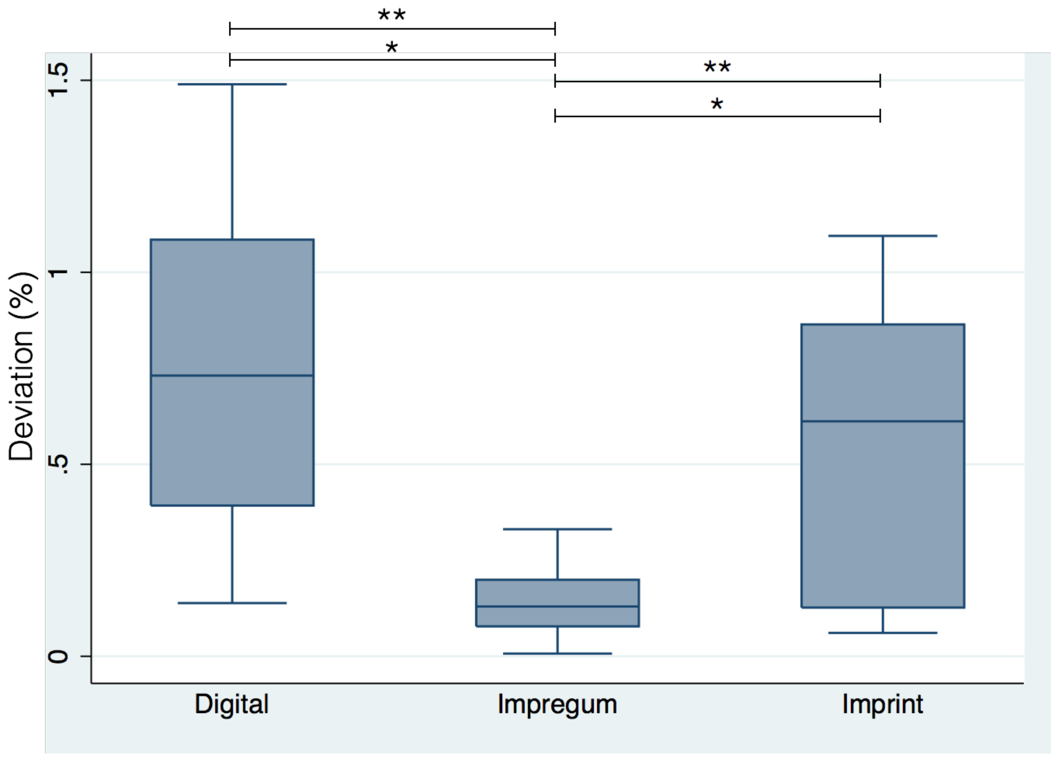

Figure 5-10: Boxplots representing the angular deviation of each impression-making group as a percentage of the reference in the overall analysis. Asterisk: p<0.05 (in variability values), double asterisk: p<0.05 (in mean values).

According to each implant analog's position analysis and the percentage expression, statistically significant differences in mean values were found between Impregum and IOS, Imprint and IOS, Imprint and Impregum for the distance "1-3" and between Impregum and IOS for the distance "1-4". No statistically significant differences were found in variability among all three impression-making methods for all distances (Table 5-9, 5-10; Appendix: Figure 11-13, 11-14).

Table 5-9: Comparison of mean values in angular deviation for each analyzed interval

Impressioning Group	Distance	Difference in angle (˚)	p-value
Impregum vs. IOS	1-2	-0.13	0.103
Imprint vs. IOS	1-2	-0.02	0.715
Imprint vs. Impregum	1-2	0.11	0.085
Impregum vs. IOS	1-3	-0.38	< 0.0001
Imprint vs. IOS	1-3	-0.14	0.039
Imprint vs. Impregum	1-3	0.24	0.003
Impregum vs. IOS	1-4	-0.21	0.029
Imprint vs. IOS	1-4	-0.08	0.278
Imprint vs. Impregum	1-4	0.13	0.09

˚ = degrees

Table 5-10: Comparison of variability and its percentage expression in the angle deviation of each analyzed interval

Material	Distance	Datasets	Mean (˚)	SD (˚)	Mean (%)	SD (%)	p-value
IOS	1-2	5	0.16	± 0.08	0.42	± 0.21	0.221
Impregum	1-2	5	0.04	± 0.03	0.1	± 0.07	
Imprint	1-2	5	0.14	± 0.13	0.36	± 0.32	
IOS	1-3	5	0.45	± 0.1	1.12	± 0.25	0.261
Impregum	1-3	5	0.07	± 0.04	0.18	± 0.1	
Imprint	1-3	5	0.31	± 0.13	0.76	± 0.33	
IOS	1-4	5	0.27	± 0.11	0.65	± 0.26	0.277
Impregum	1-4	5	0.06	± 0.05	0.15	± 0.11	
Imprint	1-4	5	0.19	± 0.15	0.45	± 0.36	

˚ = degrees

5.2.3 Reference Model 1 versus Model 2

The datasets of the reference model 1 (four straight implants) and model 2 (two straight and two tilted implants) were compared regarding angle deviation for all three impression-making approaches. Statistically significant differences in overall variability between model 1 (15 datasets) and model 2 (15 datasets) were found in the impression-making group with Imprint (p=0.004), but not with IOS (p=0.168) or Impregum (p=0.127). Nevertheless, the percentage expression showed statistically significant differences in all three groups: IOS (p=0.002), Impregum (p=0.008), and Imprint (p=0.0001).

Similar to the data of variability, the overall mean values showed a statistically significant difference only for the Imprint group (p=0.018). However, the percentage expression showed significant differences in all the groups: IOS (p<0.0001), Impregum (p=0.003), Imprint (p<0.0001) (Figure 5-11, 5-12).

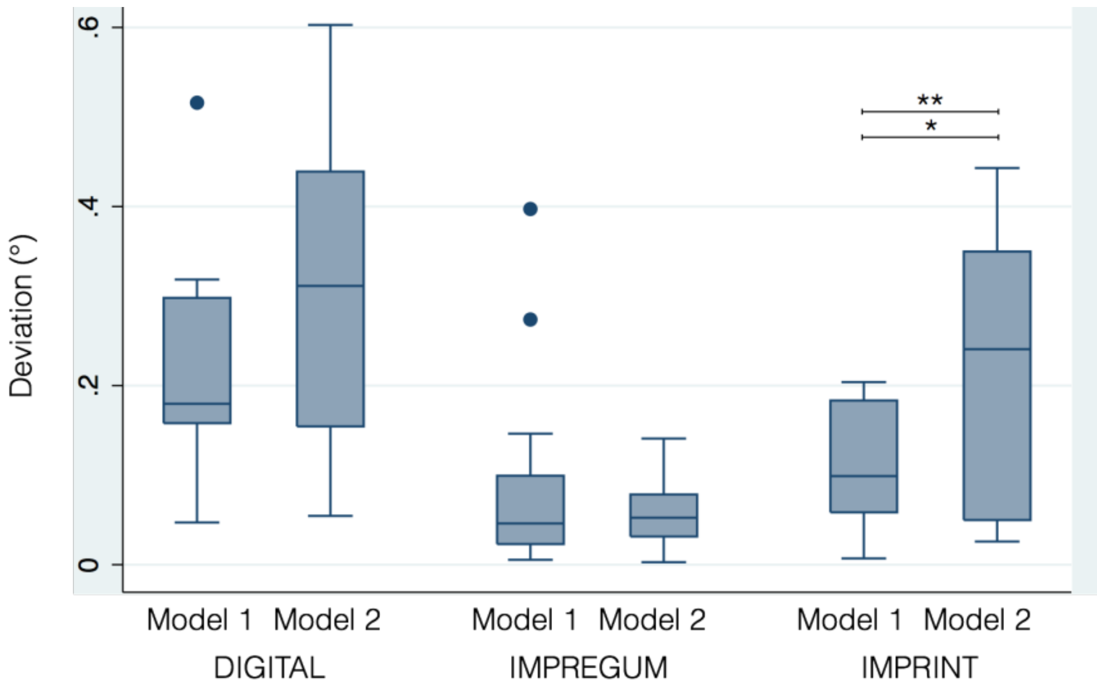

Figure 5-11: Boxplots representing the angle deviation in the reference model 1 and model 2 for all impression-making methods. Asterisk: p<0.05 (in variability values), double asterisk: p<0.05 (in mean values).

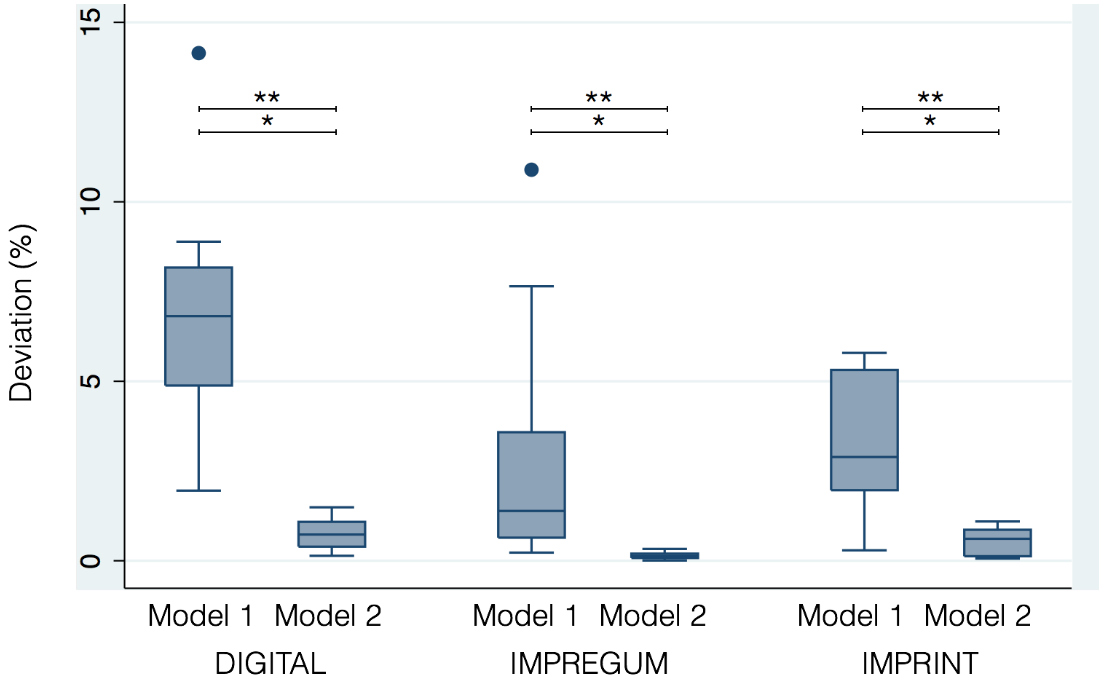

Figure 5-12: Boxplots representing angle deviation as a percentage of the reference across all impression-making methods and both reference models. Asterisk: p<0.05 (in variability values), double asterisk: p<0.05 (in mean values).

The statistical analysis of variability between reference model 1 and model 2 including all three impression making methods showed no statistically significant difference for any of the intervals between each implant analog. However, the percentage expression showed significant differences in the group of Impregum (distance "1-2") and Imprint (distance "1-3").

According to the one-way ANOVA analysis, significant differences in mean values were found in the group of IOS (distance "1-3") and Imprint (distance "1-3"). Nevertheless, the percentage expression of differences in mean values were found to be significant in all impression making groups for all the distances, except with Impregum for the distances "1-3", "1-4" (Table 5-11; Appendix: Figure 11-15 – 11-20).

Table 5-11: Comparison of variability and mean values in the angle deviation of each analyzed interval in both reference models

Material	Distance	p-value (variability)	p-value (variability %)	p-value (mean)	p-value (mean %)
IOS	1-2	0.468	0.085	0.523	0.001
Impregum	1-2	0.48	0.013	0.834	0.049
Imprint	1-2	0.237	0.063	0.273	0.027
IOS	1-3	0.855	0.115	0.003	0.001
Impregum	1-3	0.585	0.294	0.874	0.159
Imprint	1-3	0.427	0.019	0.025	0.043
IOS	1-4	0.981	0.114	0.653	0.001
Impregum	1-4	0.301	0.146	0.249	0.063
Imprint	1-4	0.181	0.066	0.514	0.001

6 Discussion

This *in vitro* study investigated the accuracy of implant impression making of computer-aided vs. conventional approaches and straight vs. tilted implants in a standardized setting. The results showed some statistically significant differences in variability and mean deviations between the different methods and different reference models (reference model 1 – four straight implants, reference model 2 – two straight and two tilted implants). Nevertheless, the obtained deviations in the inter-implant distance and angle seem to be clinically irrelevant. However, there is no data available in the literature that generally defines clinically acceptable error in distance and angulation.

6.1 Discussion of materials and methods

The selection of an appropriate material for reference model fabrication is barely discussed in the dental literature. Various materials have diverse characteristics, which must correspond to the specifications of the chosen investigation. Materials such as stainless steel (Ender & Mehl, 2013b; Seelbach et al., 2013), cobalt-chromium alloy (Ender & Mehl, 2011), stone (Papaspyridakos et al., 2015; van der Meer et al., 2012), polyurethane (Patzelt, Bishti, et al., 2014; Patzelt, Emmanouilidi, et al., 2014), epoxy resin (Lin, Harris, et al., 2015), and pink acrylic resin (Gimenez et al., 2013; Gimenez, Ozcan, Martinez-Rus, & Pradies, 2014) were used to manufacture the reference models in previous studies. In order to find an appropriate material for a recent investigation, the focus was put on the features of the aforementioned materials.

Metal-based models have favorable mechanical and physical properties, however the light reflection from surface features (Patzelt, Emmanouilidi, et al., 2014) and the complexity of placing dental implants are unfavorable. These adverse characteristics resulted in the avoidance of metal as the fabrication material in the present study.

Dental stone was another option. However, stone models are brittle and prone to absorb water, and therefore sensitive to humidity (Patzelt, Emmanouilidi, et al., 2014). On the other hand, the intraoral scanner can more easily capture the structure due to the stone models' matt surface (Gimenez et al., 2013).

Polyurethane and epoxy resin are highly precise materials, and would be advantageous relative to stone models. However, polyurethane is sensitive to water uptake and temperature-related distortions (ZenduraDentalTeam, 2012). On the other hand, epoxy resin is a very stable material, but susceptible to UV radiation (NilsMalmgrenAB, 2015).

As for PMMA, the material is dimensionally stable, has a high mechanical strength, low moisture- and water-absorbing capacity with acceptable thermal stability and is resistant to direct sunlight exposure (Koleva, 2014).

Most intraoral scanners on the market utilize one of several different non-contact optical technologies: confocal microscopy (e.g. iTero), optical coherence tomography (e.g. E4D), photogrammetry (e.g. PICcamera® (PICdental, Madrid, Spain) (Penarrocha-Oltra, Agustin-Panadero, Bagan, Gimenez, & Penarrocha, 2014), active and passive stereovision/triangulation (e.g. CEREC AC Bluecam), interferometry (e.g. DPI-3D), and phase shift principles (Logozzo et al., 2011; Logozzo et al., 2013). The IOS used in the present investigation is based on a wavefront sampling technology, which, together with a special acquisition speed, permits more sampling positions and a theoretically more accurate scan (Figerio, 2006). The True Definition Scanner projects the image on a sensor through a lens system. If the distance from the lens to the object corresponds to a focal length of the lens, the image is in focus; if not, the image is fuzzy and the distance between the lens and the object is calculated through a mathematical formula (Gimenez et al., 2013). The control of the focal distance during the scanning process helps to control the precision and accuracy of the whole scan.
The True Definition Scanner is also a video-based system with larger overlapping areas of every taken image (Patzelt, Bishti, et al., 2014), which does not need any calibration before the scanning process. This allows for faster application of the equipment and more accurate image stitching. Nevertheless, there is no information in the literature regarding which intraoral scanner technology is the most precise.

Very light dusting with a scanning powder is necessary with the True Definition IOS to prevent surface reflections, enhance data acquisition, and improve the stitching of the images. The main component of the scanning powder spray used here is titanium dioxide. However, there is no information about the effect of the scanning powder on human health, a point of particular interest since it could be inhaled into the lungs or swallowed into the stomach during the application process (Patzelt et al., 2013).
There are several studies in the literature analyzing the influence of scanning powder application on the accuracy of the scan. It was stated that computer-aided impression making without surface pretreatment may reduce the risk of powdering errors and, therefore, scanning distortions (Ender & Mehl, 2013b). Furthermore, it was also found that the most commonly documented error during the digital scanning process is an irregular powder arrangement, which contributed to 264 errors in 1251 images (21.1%) (J. H. Kim et al., 2015).

In contrast, a recent laboratory study utilized and compared four different IOSs (CEREC AC Bluecam, Lava C.O.S., iTero, and Zfx IntraScan) and found no evidence that scanning powder negatively effects the dimensional object accuracy (Patzelt et al., 2013). A further investigation also failed to find any statistically significant negative powdering effects on the marginal accuracy of the restorations (da Costa, Pelogia, Hagedorn, & Ferracane, 2010).

The IOS used in our study does not require coating, but rather a very light dusting of scanning powder. Lately, it has been suggested that the coating is a sensitive procedure, heavily dependent on the operator's experience (Dehurtevent et al., 2015). It was showed that an operator, who applies CAD/CAM systems daily (experienced operator), achieves a more homogeneous and thinner powder coating than an inexperienced one. Nevertheless, it seems that dusting is an easier procedure to perform compared to coating, and therefore the risk for powdering error is smaller.
The effect of operator experience was also analyzed regarding the scanning quality. The *in vitro* study (Gimenez et al., 2014) concluded that even though the inexperienced operator takes more time to scan, accuracy does not necessarily depend on experience. On the contrary, another study from the same authors (Gimenez et al., 2013) showed that the operator's experience does play a role in scanning accuracy, but conclude that 15 scans are enough to achieve the learning curve. The operator in the present study had an experience of 30 scans before the investigation started.

Since there are no studies regarding the most accurate scanning protocol for an edentulous jaw with implants, the manufacturer of the IOS from our investigation was contacted. Following the manufacturer's suggestion, the double gingival scanning method was applied as the most precise known scanning strategy for a digital implant impression-making procedure.

This *in vitro* study attempted to provide practical information about the possibility of manufacturing a screw-retained framework on multiple implants using a digital intraoral impression. It was decided to choose implants with a favorable design that could be accurately measured by a reference scanner (Gimenez et al., 2014). For this reason, Osseotite® 2 Certain® implants were used in the present study. They have a parallel-walled internal connection and two flat surfaces, which could be accurately identified and measured with the CMM (Gimenez et al., 2013).
The high-precision PEEK scanbodies (milled by Createch Medical) have a cylindrical form and were chosen due to their favorable mechanical and chemical properties. They are 8 mm in height and did not provide any rotational information about the implants. However, such information would not be necessary to manufacture a CAD/CAM framework on multiple implants because the prosthesis itself is established without an anti-rotation lock.

To be able to assess the accuracy of the IOS and conventional elastomer materials included in the present investigation, it was also necessary to choose a precise reference-measuring device. Following the experience of previous studies (Del Corso et al., 2009; Gimenez et al., 2013, 2014; Jemt & Hjalmarsson, 2012), the tactile coordinate measuring machine (CMM), which has a certified accuracy of 1.9 + 3L/1000 µm, was used for this purpose. The CMM was located in a room under highly controlled conditions (e.g. temperature, humidity, vibration) to ensure the appropriate environment and stability of the device. The important aspect of the measuring approach with CMM is that the maximum measuring error does not accumulate.

Many studies similar to this one used various 3D laser scanners, for instance: the proprietary noncontact laser scanner (Cagenix; Cagenix Inc, Memphis, USA) with a scanning gauge accurate to 1 µm (Lin, Harris, et al., 2015); the Laserscan 3D Pro (Willytec; Munich, Germany) with an accuracy of 12 µm (Mehl, Ender, Mormann, & Attin, 2009; Mehl, Gloger, Kunzelmann, & Hickel, 1997); the laser-measuring machine (LK, Integra; Metris Metrology Solutions, Leuven, Belgium) with a claimed accuracy of 10-15 µm (Eliasson & Ortorp, 2012); and the simedaScan (Imetric 3D GmbH; Courgenay, Switzerland), which, according to the manufacturer's specifications, was accurate to < 20 µm (Patzelt, Bishti, et al., 2014).

The characteristics of the chosen reference scanner may have an influence on the objectivity of the data and interpretation of the results.

Since a conventional impression-making procedure was also included in our investigation, the literature was reviewed regarding the most advisable conventional materials for multiple-implant impression. A recent literature review showed that polyether and VPS are the most accurate impression materials for edentulous multiple-implant situations (Baig, 2014). Another review likewise supported this conclusion and asserted that a condensation silicone, polysulfide, reversible and irreversible hydrocolloid, or plaster have no improved accuracy in comparison to a polyether or VPS impression (H. Lee et al., 2008). Regarding the aforementioned literature analyses, the polyether and VPS were also applied in the present study, as the most appropriate materials for the implant impression-making procedure.

The additional question of whether or not to splint multiple implants before making an impression was discussed in different studies. An important aspect related to the multiple implants, splinting, and impression-making procedure is whether the implants are placed parallel to one another. If the splinted implants have distinct differences in angle, withdrawing the impression from the mouth might be difficult or even impossible (Lin, Harris, et al., 2015; Malo, de Araujo Nobre, Lopes, Francischone, & Rigolizzo, 2012). In certain cases, even if such implants are not splinted, the risk of distorting the impression material while removing it from the mouth is high. It is particularly complicated with higher numbers of implants (Akalin, Ozkan, & Ekerim, 2013; H. Lee et al., 2008) (i.e. four or more implants (Mpikos et al., 2012)) and if the closed-tray impression technique is chosen (Barrett, de Rijk, & Burgess, 1993).

The accuracy of conventional impressions with splinted and non-splinted implants at variable angles was investigated in an *in vitro* study (Filho et al., 2009). It was stated that tilted implants (65˚) presented relatively high angular deviations with a mean value of 0.817˚. In comparison, the non-tilted implants (90˚) showed a mean angle deviation of 0.282˚. The difference between tilted and straight implants was statistically significant in the non-splinted and splinted groups, except in the group where prefabricated acrylic bars were used to splint the implants. Another study concluded that "the more perpendicular the implant analog angulation is in relation to the horizontal surface, the more accurate the impression is" (Assuncao, Filho, & Zaniquelli, 2004). Nevertheless, there are also other investigations in which no significantly negative influence of the tilted implants was found (Choi, Lim, Yim, & Kim, 2007; Conrad, Pesun, DeLong, & Hodges, 2007).

The conventional implant impression in the present investigation was performed without splinting and applying a 1-step open-tray impression. The splinting of 40-45˚ tilted implants would lead to an impression that cannot be removed from the mouth.

6.2 Discussion of results

The number of studies investigating the accuracy of different intraoral scanners is increasing. Most of the studies have been designed using study models with teeth and focusing on trueness and precision measurements. While many studies exist testing the accuracy of different conventional implant impression-making methods, there is a lack of studies evaluating the accuracy of digital implant impression making.

Two recent *in vitro* studies (Gimenez et al., 2013, 2014) evaluated the accuracy of digital implant impression making with the Lava C.O.S. (3M ESPE, St Paul, MN, USA) and the iTero (Cadent Inc, Carlstadt, USA) IOSs. Both studies used the same resin study model – an edentulous mandible with six implants. Five distances between each implant were measured and compared to the reference dataset.

In the group of experienced operators, the mean deviation found with the Lava C.O.S. ranged between 11.02 ± 28.12 µm and 45.02 ± 37.31 µm; in the group of inexperienced operators, the range was between -4.37± 73.47 µm and 39.70 ± 54.18 µm. In the study with the iTero, the mean deviation ranged between 14.3 ± 25.6 µm and -32 ± 216.1 µm and the results were not separated with regard to the operator's experience. Both studies demonstrated that an implant angulation of 30˚ did not have any significantly negative impact on the distance deviation.

The mean distance deviation in our study using the True Definition Scanner ranged between -6.5 ± 15.88 µm and 23.66 ± 4.24 µm (reference Model 1) and between 39.51 ± 5.51 µm and 63.91 ± 10.12 µm (reference Model 2). These findings are in agreement with the results obtained with the Lava C.O.S. The Lava C.O.S., like the True Definition Scanner, is based on active wavefront sampling technology. The distance deviation of both IOSs did not exceed the threshold of 100 µm. However, the results of the iTero were more variable than either of the other scanners. This could be explained by the different scanning technology of the iTero, which uses confocal laser scanning with a red light beam. Moreover, four implants were scanned in the present investigation, whereas six implants were used in the studies of Gimenez et al., 2013, 2014. This might also play a role, since it is known that a longer scanning track leads to increased scanning error (Gimenez et al., 2014).

Regarding implant angle, the present investigation showed a statistically significant distance deviation between straight and tilted dental implants. Statistically significant mean distance deviation was found in the group of IOS for all three distance intervals. This diversity might be explained by the bigger implant angle (of 40-45˚) in our study than it was in the studies by Gimenez et al., 2013, 2014. Nevertheless, the clinical relevance of such statistically significant differences between straight and tilted dental implants found in our investigation is unclear.

Three triangularly-placed implants in a full arch mandibular stone model were investigated in an *in vitro* study (van der Meer et al., 2012). Three different IOSs, the Lava C.O.S., the iTero, and the CEREC AC Bluecam (Sirona Dental Systems GmbH, Bensheim, Germany) were used to digitize the whole arch with teeth and implants. Two distances between each implant were measured and compared to the reference dataset. The Lava C.O.S. produced a mean distance deviation between the implants of 14.6 ± 12.7 µm to 23.5 ± 14.2 µm, the iTero of 61.1 ± 53.9 to 70.5 ± 56.3 µm, and the CEREC AC Bluecam of 79.6 ± 77.1 µm to 81.6 ± 52.5 µm. Regarding the error in the measured implant angle, the Lava C.O.S. generated a mean angle deviation between 0.2 ± 0.04˚ and 0.47 ± 0.14˚; iTero between 0.35 ± 0.34˚ and 0.42 ± 0.17˚; and CEREC AC between 0.63 ± 0.55˚ and 0.44 ± 0.32˚. No statistical difference was found among the three groups.

The mean angle deviation (of 0.13 ± 0.06° to 0.31 ± 0.13° in Model 1; of 0.16 ± 0.08° to 0.45 ± 0.1° in Model 2) found with the True Definition Scanner in our study seems to be in agreement with the aforementioned study. Nevertheless, the discrepancies in the distance deviation might be

attributed not only to the different scanning technologies (iTero and CEREC AC Bluecam), but also to the different study model design.
The reference model in the study of van der Meer et al., 2012 was fabricated from dental stone. Dental stone, in comparison to resin, is a matt material and can be more easily captured by the IOS (Gimenez et al., 2013). Furthermore, a larger amount of reference points was ensured through the presence of teeth in the study model. Thus, the digital impression of the edentulous model solely with implants might be more complicated and less accurate (Andriessen et al., 2014). However, scanning straight implants is easier than tilted ones. Therefore, in comparison to our study, the slightly better results presented in the aforementioned study with the Lava C.O.S might be affected by some or all of the above-mentioned factors.

Another recent *in vitro* study is the only published study comparing the accuracy of digital and conventional implant impressions for completely edentulous patients (Papaspyridakos et al., 2015). The edentulous mandibular dental stone model with five implants was analyzed. The Trios IOS (3shape, Copenhagen, Denmark) was used for a digital impression, and polyether material was used for a conventional impression. In contrast to the CMM and contact scanner technology used in the previously mentioned studies, the 6-µm precision extraoral scanner (IScan D103i, Imetric) was chosen as the reference scanner. The median overall deviation of the implants found in conventional impression making when the implants were splinted was 7.42 µm (5.28-10.88 µm). Using a non-splinted conventional impression technique, the deviation was 17.56 µm (13.19-76.49 µm), and digitizing the reference model with Trios, the deviation was 19.38 µm (11.54-26.21 µm). It was concluded that the digital impressions are as accurate as the conventional ones, and significant deviation was found only between the non-splinted conventional implant impression making and the control group, i.e. reference data. It was also stated that implant angles of 10˚ and 15˚ did not negatively affect the accuracy of implant impressions, which is in agreement with the studies of Gimenez et al., 2013, 2014.
Our investigation found an overall mean distance deviation of the conventional non-splinted impressions of 12.22 ± 16.93 µm (reference Model 1) and 19.78 ± 21 µm (reference Model 2) for polyether, and of 12.74 ± 12.5 µm (reference Model1) and 4.87 ± 21.34 µm (reference Model 2) with PVS. There was no statistically significant difference found between impressions performed with the True Definition Scanner, polyether, and PVS materials in the reference Model 1. Nevertheless, the overall mean distance deviation of all three impression-making approaches differed significantly in the reference Model 2.
Further analysis between straight and tilted dental implants in the present study showed statistically significant differences in angle deviation in the group of PVS (distance “1-3”). Nevertheless, there

was no significant difference in angle or distance deviation in the group of polyether. This finding corroborates the results of Papaspyridakos et al., 2015.

However, there is one important methodological difference that does not allow a direct comparison of the study of Papaspyridakos et al., 2015 with our study and the other before mentioned ones; namely, the difference in the accuracy assessment method: the best-fit algorithm (Papaspyridakos et al., 2015) versus the “zero-method” (the present investigation; Gimenez et al., 2013, 2014; van der Meer et al., 2012).

The best-fit algorithm or, in other words, general overlapping of the reference and the test objects was basically used in most of the studies (Ender & Mehl, 2011, 2015; Grunheid et al., 2014; Guth et al., 2013; Lin, Harris, et al., 2015; Mehl et al., 2009; Nedelcu & Persson, 2014; Papaspyridakos et al., 2015; Patzelt, Bishti, et al., 2014; Patzelt, Emmanouilidi, et al., 2014; Patzelt et al., 2013; Vandeweghe et al., 2015), which analyzed the accuracy (with or without precision) of the computer-aided impression making method. The superimposition of two datasets, i.e. the reference and the test, means the superimposition of two different clouds of points. Each cloud has a different reference system, for instance, the CMM (or other reference scanner) versus the IOS. Finding the best-fitting overlap of clouds with a different reference leads to the proper alignment, with the difference between the clouds considered to be the measuring uncertainty.

The other methodological alternative, the so-called “zero method” (Jemt & Hjalmarsson, 2012), considers the center point of the chosen implant as the reference and obtains the linear distances or angulations between the implants in the certain model. This method avoids an alignment of the datasets, as in the best-fit algorithm, and provides the exact deviation in distance or angulation. Such measurements could not be broken down into the x-, y-, z-coordinates of the other reference system (Andriessen et al., 2014; van der Meer et al., 2012), because it would introduce the aforementioned error of the averaging process, while matching different data clouds. However, it compares the exact distances and angles (found with the coordinate measurements) by mathematical subtraction and without manipulating the data.

The recent study (Lin, Harris, et al., 2015) compared the accuracy of the definitive stone and milled polyurethane casts. The casts were manufactured after conventional (with polyvinyl siloxane material) and digital (with iTero IOS) impression making. The dentate epoxy resin mandible with two implants, placed parallel or angled (15˚, 30˚, and 45˚) was used. Virtual mating was performed to analyze the accuracy of both implant impression techniques. The results showed that the polyurethane casts had larger deviations in angular and distance measurements compared to the stone casts, regardless of the different implant divergence. However, it could not be concluded that the computer-aided impression making is less accurate than conventional. The error could have been caused during the CAD/CAM milling process of the definitive cast and/or by inserting implant analogs manually. Hence, it was concluded that the digital pathway does not lead to less accurate digital impressions, but to less accurate definitive cast production, which is, however, more accurate when the implants diverge more. It must be also said that the implant angulation had no negative impact on conventional stone casts, manufactured using an open tray non-splinted implant level impression.

Another study (S. J. Lee et al., 2014) compared the accuracy of conventionally fabricated gypsum casts and digitally milled polyurethane models. The results, however, were not in agreement with the previously mentioned study. It was found that the two model fabrication methods, after conventional and computer-aided impression making procedures, have comparable accuracy. Such diversity of the results in both studies might be influenced by the different implant quantity and position in the reference model. In their study, Lee et al., 2014 placed only one straight implant between the teeth, while Lin et al., 2015 analyzed two implants with different angulation in an edentulous posterior region of the dentate mandible.

There is the only published *in vivo* study until now, which analyzed the accuracy of the True Definition intraoral scanner (Boeddinghaus et al., 2015). Two other IOSs (CEREC AC Omnicam and Trios) and a conventional impression-making method (with vinyl polyether silicone material) were added in the study. The conventional and digital impressions with all three IOSs were performed on 49 teeth in 24 patients. Zirconia copings were manufactured regarding each dataset and the marginal gap was evaluated. The results showed an 88 µm (median) marginal gap for the True Definition scanner, 112 µm for Trios, 149 µm for CEREC AC Omnicam, and 113 µm for conventional impression making. The authors concluded that the digital intraoral impression-making procedure could be considered as an alternative to the conventional, if the consecutive digital workflow can be followed.

There are also three case reports and one *in vivo* study in the literature to date analyzing the clinical capacity and accuracy of the digital intraoral impression-making procedure for an edentulous jaw with dental implants. The IOS Lava C.O.S. was used in a recent case report (Moreno, Gimenez, Ozcan, & Pradies, 2013). Six mandibular dental implants were scanned in one patient. The detailed clinical protocol, starting with the computer-aided impression making procedure, CAD/CAM metal framework manufacturing, and clinical/laboratory application procedures were presented. The report showed that it is possible to perform an accurate digital impression of multiple implants *in vivo*. However, further clinical investigations are needed to approve the consistency of the results.

Furthermore, the same conclusion was likewise presented in other clinical case reports (Lin, Chou, Metz, Harris, & Morton, 2015; Lin, Harris, Zandinejad, & Morton, 2014). The iTero IOS was applied for a patient with six dental implants in the maxilla. The authors suggested verification of the implant position after the intraoral digitation. A laboratory manufactured implant-splinting device might be applied. However, it was concluded that further development of intraoral scanners and CAD/CAM systems is needed to be able to avoid such additional appliances in the future.

The only *in vivo* study up to now comparing intraorally digitized scanbodies with conventionally fabricated and extraorally scanned casts was published in 2014 (Andriessen et al., 2014). This clinical study included 25 patients with two dental implants in each edentulous mandible and applied the iTero IOS. It assessed the accuracy using the "zero-method" described above. Maximum thresholds of 100 µm for a clinically acceptable distance error and 0.4˚ for an angulation error were set in the study. The mean distance error was found to be 226 µm and the mean absolute angulation error was 2.582˚. The authors concluded that using the intraoral impression making procedure would not be possible to produce a passive superstructure on two implants because of the large errors in the distance and angulation. The explanation for the unreliable intraoral scans might be a sparse quantity of the reference points caused by mucosa and a lack of other anatomical landmarks.

Since some aforementioned *in vitro* studies (Del Corso et al., 2009; Karl et al., 2012; Papaspyridakos et al., 2015) showed that the digital implant impression is a valid alternative to the conventional procedure, the results are not unanimous. The *in vivo* study (Andriessen et al., 2014) showed, in contrast, that the accuracy of the intraoral scanning procedure does not substitute the conventional method and could not ensure the manufacturing of a passive-fitting prosthesis.
Some significant differences between digital and conventional approaches were likewise found in the present investigation. The results might be influenced by the non-splinted impression making technique (Papaspyridakos et al., 2014) and stone cast manufacturing (Del Corso et al., 2009) during the conventional procedures. Furthermore, the inaccuracies of the digital method might be caused by the IOS technology (Patzelt, Emmanouilidi, et al., 2014), scanning method (Ender & Mehl, 2013b), scanning powder application (Ender & Mehl, 2013b; J. H. Kim et al., 2015), IOS wand position relative to the object, and hand shaking (Mada et al., 2003). Moreover, the operator's ability and mechanical tolerances between each scanbody (digital approach) or pick up coping (conventional approach) connected to the implant analog might add additional accuracy error (S. Kim et al., 2006). At last, it has to be also taken into consideration that the *in vitro* environment does not fully correspond to *in vivo* conditions, such as the presence of saliva, patient movements, mobile areas of mucosa, or difficulties in accessing some areas in the mouth for the correct digital or conventional impression (Patzelt et al., 2013).

7 Conclusion

The present investigation demonstrated certain deviations in the inter-implant distance and implant angulation, applying computer-aided and conventional impression making approaches. However, the effect of tilted implants and the identified inaccuracies with both impression-making methods seem to be clinically irrelevant.

Based on the results of this study, both computer-aided and conventional impression-making approaches (with polyether and VPS materials) are applicable for straight and tilted dental implants and could be used for the fabrication of multiple implant restorations. Nevertheless, the *in vivo* verification is necessary.

8 Summary

This study evaluates the accuracy of computer-aided and conventional impression-making procedures of straight and tilted dental implants in a standardized *in vitro* setting.

Two edentulous acrylic resin study models with four interforaminally positioned implant analogs were fabricated. Model 1 had four straight and Model 2 had two straight and two laterally tilted implant analogs of 40-45˚. Both study models were scanned digitally (n=5) with the True Definition Scanner (software version 4.0.3.1, 3M ESPE, St. Paul, MN, USA). Additionally, conventional impressions with polyether (Impregum™ Penta™ Medium Body, 3M ESPE, St. Paul, MN, USA) (n=5) and vinyl polysiloxane (VPS) (Imprint™ 4 Penta™ Heavy and Regular, 3M ESPE, St. Paul, MN, USA) (n=5) were performed. An industrial coordinate measuring machine (CMM) (Createch Medical S.L., Mendaro, Spain) was used as the reference scanner to generate reference datasets for both study models. The collected data of the digital and conventional impressions were analyzed in terms of deviation in implant distance and angle. For accuracy assessment, the "zero-method" was applied.

The results showed the overall distance deviation with IOS 9.46 ± 16.04 µm (Model 1), 35.78 ± 24.22 µm (Model 2); with Impregum 12.22 ± 16.93 µm (Model 1), 19.78 ± 21 µm (Model 2); with Imprint 12.74 ± 12.5 µm (Model 1), 4.87 ± 21.34 µm (Model 2). Statistically significant mean differences ($p<0.05$) were found among all three impression-making groups in Model 2, as well as between Model 1 and Model 2 in the IOS group.
The overall angle deviation with IOS was 0.17 ± 0.14˚ (Model 1), 0.22 ± 0.19˚ (Model 2); with Impregum 0.07 ± 0.1˚ (Model 1), 0.04 ± 0.04˚ (Model 2); with Imprint 0.08 ± 0.07˚ (Model 1), 0.16 ± 0.16˚ (Model 2). Statistically significant mean differences ($p<0.05$) were found between IOS and Impregum, IOS and Imprint in Model 1; between IOS and Impregum, Impregum and Imprint in Model 2; and between Model 1 and Model 2 in the group of Imprint.

In this *in vitro* study, the accuracy of the computer-aided and conventional impression making approaches for straight and tilted dental implants seems to be clinically acceptable and can therefore be considered applicable for full-arch, multiple implant restorations. Nevertheless, the *in vivo* verification is necessary.

9 Zusammenfassung

Das Ziel der vorliegenden standartisierten in vitro Untersuchung war die Genauigkeit der digital und konventionell abgeformten Implantate zu bewerten.

Zwei zahnlose Kunststoffmodelle wurden mit vier Implantaten in der Interforaminalregion hergestellt. Model 1 hatte vier gerade Implantate und Model 2 zwei gerade und zwei angulierte Implantate von 40-45˚. Beide Modelle wurden mit dem True Definition Scanner digitalisiert (n=5) und mit zwei Abformmaterialien (Impregum (n=5) und Imprint (n=5)) konventionell abgeformt. Eine Koordinaten-Messmaschine wurde angewendet um die Referenz Datensätzen der beiden Modelle zu erstellen. Alle digital und konventionell erhaltenen Werte wurden hinsichtlich Abweichungen in Abstand und Angulation zwischen den Implantaten analysiert und ausgewertet. Für die Beurteilung der Genauigkeit wurde die so genannte „zero-method“ angewendet.

Die Gesamtabweichung bezüglich des Abstands war 9.46 ± 16.04 µm (Model 1), 35.78 ± 24.22 µm (Model 2) mit IOS; 12.22 ± 16.93 µm (Model 1), 19.78 ± 21 µm (Model 2) mit Impregum; 12.74 ± 12.5 µm (Model 1), 4.87 ± 21.34 µm (Model 2) mit Imprint. Die Datenanalyse ergab statistisch signifikante Unterschiede ($p<0.05$) der mittleren Werte zwischen allen drei Gruppen für Model 2 und zwischen Model 1 und Model 2 in der Gruppe der digitalen Abformung.
Die Gesamtabweichung der Angulationsmessung lag für die digitale Abformung bei 0.17 ± 0.14˚ (Model 1), 0.22 ± 0.19˚ (Model 2), für Impregum bei 0.07 ± 0.1˚ (Model 1), 0.04 ± 0.04˚ (Model 2) und für Imprint bei 0.08 ± 0.07˚ (Model 1), 0.16 ± 0.16˚ (Model 2) mit Imprint. Die Datenanalyse ergab statistisch signifikante Unterschiede ($p<0.05$) der mittleren Werte zwischen IOS und Impregum, IOS und Imprint in Model 1, zwischen IOS und Impregum, Impregum und Imprit in Model 2 und zwischen Model 1 und Model 2 in der Gruppe von Imprint.

Es wurde festgestellt, dass digitale und konventionelle Abformverfahren für gerade und angulierte Implantate ein akzeptables Maß der Genauigkeit zeigten und daher für ganz-Kiefer restaurative Verfahren auf mehreren Implantaten geeignet sind. Dennoch ist die *in vivo* Überprüfung notwendig.

10 References

Adell, R., Lekholm, U., Rockler, B., & Branemark, P. I. (1981). A 15-year study of osseointegrated implants in the treatment of the edentulous jaw. *Int J Oral Surg, 10*(6), 387-416.

Akalin, Z. F., Ozkan, Y. K., & Ekerim, A. (2013). Effects of implant angulation, impression material, and variation in arch curvature width on implant transfer model accuracy. *Int J Oral Maxillofac Implants, 28*(1), 149-157.

Andriessen, F. S., Rijkens, D. R., van der Meer, W. J., & Wismeijer, D. W. (2014). Applicability and accuracy of an intraoral scanner for scanning multiple implants in edentulous mandibles: a pilot study. *J Prosthet Dent, 111*(3), 186-194.

Assuncao, W. G., Filho, H. G., & Zaniquelli, O. (2004). Evaluation of transfer impressions for osseointegrated implants at various angulations. *Implant Dent, 13*(4), 358-366.

Att, W., Bernhart, J., & Strub, J. R. (2009). Fixed rehabilitation of the edentulous maxilla: possibilities and clinical outcome. *J Oral Maxillofac Surg, 67*(11 Suppl), 60-73.

Baig, M. R. (2014). Accuracy of impressions of multiple implants in the edentulous arch: a systematic review. *Int J Oral Maxillofac Implants, 29*(4), 869-880.

Barrett, M. G., de Rijk, W. G., & Burgess, J. O. (1993). The accuracy of six impression techniques for osseointegrated implants. *J Prosthodont, 2*(2), 75-82.

Boeddinghaus, M., Breloer, E. S., Rehmann, P., & Wostmann, B. (2015). Accuracy of single-tooth restorations based on intraoral digital and conventional impressions in patients. *Clin Oral Investig*.

Branemark, P. I., Hansson, B. O., Adell, R., Breine, U., Lindstrom, J., Hallen, O., & Ohman, A. (1977). Osseointegrated implants in the treatment of the edentulous jaw. Experience from a 10-year period. *Scand J Plast Reconstr Surg Suppl, 16*, 1-132.

Burawi, G., Houston, F., Byrne, D., & Claffey, N. (1997). A comparison of the dimensional accuracy of the splinted and unsplinted impression techniques for the Bone-Lock implant system. *J Prosthet Dent, 77*(1), 68-75.

Carr, A. B. (1991). Comparison of impression techniques for a five-implant mandibular model. *Int J Oral Maxillofac Implants, 6*(4), 448-455.

Carr, A. B., & Stewart, R. B. (1993). Full-arch implant framework casting accuracy: preliminary in vitro observation for in vivo testing. *J Prosthodont, 2*(1), 2-8.

Choi, J. H., Lim, Y. J., Yim, S. H., & Kim, C. W. (2007). Evaluation of the accuracy of implant-level impression techniques for internal-connection implant prostheses in parallel and divergent models. *Int J Oral Maxillofac Implants, 22*(5), 761-768.

Conrad, H. J., Pesun, I. J., DeLong, R., & Hodges, J. S. (2007). Accuracy of two impression techniques with angulated implants. *J Prosthet Dent, 97*(6), 349-356.

da Costa, J. B., Pelogia, F., Hagedorn, B., & Ferracane, J. L. (2010). Evaluation of different methods of optical impression making on the marginal gap of onlays created with CEREC 3D. *Oper Dent, 35*(3), 324-329.

de Avila, E. D., de Matos Moraes, F., Castanharo, S. M., Del'Acqua, M. A., & de Assis Mollo, F., Jr. (2014). Effect of splinting in accuracy of two implant impression techniques. *J Oral Implantol, 40*(6), 633-639.

Dehurtevent, M., Robberecht, L., & Behin, P. (2015). Influence of dentist experience with scan spray systems used in direct CAD/CAM impressions. *J Prosthet Dent, 113*(1), 17-21.

Del Acqua, M. A., Chavez, A. M., Castanharo, S. M., Compagnoni, M. A., & Mollo Fde, A., Jr. (2010). The effect of splint material rigidity in implant impression techniques. *Int J Oral Maxillofac Implants, 25*(6), 1153-1158.

Del Corso, M., Aba, G., Vazquez, L., Dargaud, J., & Dohan Ehrenfest, D. M. (2009). Optical three-dimensional scanning acquisition of the position of osseointegrated implants: an in vitro study to determine method accuracy and operational feasibility. *Clin Implant Dent Relat Res, 11*(3), 214-221.

DIN Deutsches Institut für Normung. Accuracy (trueness and precision) of measurement methods and results, part I: general principles and definitions (ISO 5725-1:1994). (1997). *Berlin: Beuth VerlagGmbH,*http://www.nqsz.din.de/cmd?artid=3050093&bcrumblevel=1 *&contextid=nqsz&subcommitteeid=54748182&level=tpl-art-detaila nsicht&committeeid=54739099&languageid=en. Accessed June 21, 2013.*

Eliasson, A., & Ortorp, A. (2012). The accuracy of an implant impression technique using digitally coded healing abutments. *Clin Implant Dent Relat Res, 14 Suppl 1*, e30-38.

Ender, A., & Mehl, A. (2011). Full arch scans: conventional versus digital impressions--an in-vitro study. *Int J Comput Dent, 14*(1), 11-21.

Ender, A., & Mehl, A. (2013a). Accuracy of complete-arch dental impressions: a new method of measuring trueness and precision. *J Prosthet Dent, 109*(2), 121-128.

Ender, A., & Mehl, A. (2013b). Influence of scanning strategies on the accuracy of digital intraoral scanning systems. *Int J Comput Dent, 16*(1), 11-21.

Ender, A., & Mehl, A. (2015). In-vitro evaluation of the accuracy of conventional and digital methods of obtaining full-arch dental impressions. *Quintessence Int, 46*(1), 9-17.

Faria, J. C., Silva-Concilio, L. R., Neves, A. C., Miranda, M. E., & Teixeira, M. L. (2011). Evaluation of the accuracy of different transfer impression techniques for multiple implants. *Braz Oral Res, 25*(2), 163-167.

Figerio, F. (2006). 3-dimensional surface imaging using active wavefront sampling (PhD Thesis). *Massachusetts Institute of Technology, Massachusetts, USA.* http://dspace.mit.edu/handle/1721.1/38258.

Filho, H. G., Mazaro, J. V., Vedovatto, E., Assuncao, W. G., & dos Santos, P. H. (2009). Accuracy of impression techniques for implants. Part 2 - comparison of splinting techniques. *J Prosthodont, 18*(2), 172-176.

Gimenez, B., Ozcan, M., Martinez-Rus, F., & Pradies, G. (2013). Accuracy of a Digital Impression System Based on Active Wavefront Sampling Technology for Implants Considering Operator Experience, Implant Angulation, and Depth. *Clin Implant Dent Relat Res*.

Gimenez, B., Ozcan, M., Martinez-Rus, F., & Pradies, G. (2014). Accuracy of a digital impression system based on parallel confocal laser technology for implants with consideration of operator experience and implant angulation and depth. *Int J Oral Maxillofac Implants, 29*(4), 853-862.

Grunheid, T., McCarthy, S. D., & Larson, B. E. (2014). Clinical use of a direct chairside oral scanner: an assessment of accuracy, time, and patient acceptance. *Am J Orthod Dentofacial Orthop, 146*(5), 673-682.

Guth, J. F., Keul, C., Stimmelmayr, M., Beuer, F., & Edelhoff, D. (2013). Accuracy of digital models obtained by direct and indirect data capturing. *Clin Oral Investig, 17*(4), 1201-1208.

Hariharan, R., Shankar, C., Rajan, M., Baig, M. R., & Azhagarasan, N. S. (2010). Evaluation of accuracy of multiple dental implant impressions using various splinting materials. *Int J Oral Maxillofac Implants, 25*(1), 38-44.

Howell, K. J., McGlumphy, E. A., Drago, C., & Knapik, G. (2013). Comparison of the accuracy of Biomet 3i Encode Robocast Technology and conventional implant impression techniques. *Int J Oral Maxillofac Implants, 28*(1), 228-240.

ISO International organization for Standardization. 10360-2. (2009). Geometrical product specifications (GPS). Acceptance and re-verification test for coordinated measuring machines (CMM). Part 2: CMMs used for measuring linear dimensions.

Jemt, T. (1991). Failures and complications in 391 consecutively inserted fixed prostheses supported by Branemark implants in edentulous jaws: a study of treatment from the time of prosthesis placement to the first annual checkup. *Int J Oral Maxillofac Implants, 6*(3), 270-276.

Jemt, T., & Hjalmarsson, L. (2012). In vitro measurements of precision of fit of implant-supported frameworks. A comparison between "virtual" and "physical" assessments of fit using two different techniques of measurements. *Clin Implant Dent Relat Res, 14 Suppl 1*, e175-182.

Kan, J. Y., Rungcharassaeng, K., Bohsali, K., Goodacre, C. J., & Lang, B. R. (1999). Clinical methods for evaluating implant framework fit. *J Prosthet Dent, 81*(1), 7-13.

Karl, M., Graef, F., Schubinski, P., & Taylor, T. (2012). Effect of intraoral scanning on the passivity of fit of implant-supported fixed dental prostheses. *Quintessence Int, 43*(7), 555-562.

Katsoulis, J., Muller, P., Mericske-Stern, R., & Blatz, M. B. (2015). CAD/CAM fabrication accuracy of long- vs. short-span implant-supported FDPs. *Clin Oral Implants Res, 26*(3), 245-249.

Kim, J. H., Kim, K. B., Kim, S. H., Kim, W. C., Kim, H. Y., & Kim, J. H. (2015). Quantitative evaluation of common errors in digital impression obtained by using an LED blue light in-office CAD/CAM system. *Quintessence Int*.

Kim, S., Nicholls, J. I., Han, C. H., & Lee, K. W. (2006). Displacement of implant components from impressions to definitive casts. *Int J Oral Maxillofac Implants, 21*(5), 747-755.

Kim, S. Y., Lee, S. H., Cho, S. K., Jeong, C. M., Jeon, Y. C., Yun, M. J., & Huh, J. B. (2014). Comparison of the accuracy of digitally fabricated polyurethane model and conventional gypsum model. *J Adv Prosthodont, 6*(1), 1-7.

Kim, Y., Oh, T. J., Misch, C. E., & Wang, H. L. (2005). Occlusal considerations in implant therapy: clinical guidelines with biomechanical rationale. *Clin Oral Implants Res, 16*(1), 26-35.

Koleva, M. (2014). CAE DS - Injection Moulding Materials. Poly(methyl methacrylate) (PMMA). http://www.pdfjournal.net.pdf/1ISe/polymethyl-methacrylate-pmma-tut.html.

Kravitz, N. D., Groth, C., Jones, P. E., Graham, J. W., & Redmond, W. R. (2014). Intraoral digital scanners. *J Clin Orthod, 48*(6), 337-347.

Lee, H., So, J. S., Hochstedler, J. L., & Ercoli, C. (2008). The accuracy of implant impressions: a systematic review. *J Prosthet Dent, 100*(4), 285-291.

Lee, S. J., Betensky, R. A., Gianneschi, G. E., & Gallucci, G. O. (2014). Accuracy of digital versus conventional implant impressions. *Clin Oral Implants Res.*

Lee, S. J., & Gallucci, G. O. (2013). Digital vs. conventional implant impressions: efficiency outcomes. *Clin Oral Implants Res, 24*(1), 111-115.

Lin, W. S., Chou, J. C., Metz, M. J., Harris, B. T., & Morton, D. (2015). Use of intraoral digital scanning for a CAD/CAM-fabricated milled bar and superstructure framework for an implant-supported, removable complete dental prosthesis. *J Prosthet Dent.*

Lin, W. S., Harris, B. T., Elathamna, E. N., Abdel-Azim, T., & Morton, D. (2015). Effect of implant divergence on the accuracy of definitive casts created from traditional and digital implant-level impressions: an in vitro comparative study. *Int J Oral Maxillofac Implants, 30*(1), 102-109.

Lin, W. S., Harris, B. T., Zandinejad, A., & Morton, D. (2014). Use of digital data acquisition and CAD/CAM technology for the fabrication of a fixed complete dental prosthesis on dental implants. *J Prosthet Dent, 111*(1), 1-5.

Logozzo, S., Franceschini, G., Kilpelä, A., Caponi, M., Governi, L., & Blois, L. (2011). A comparative analysis of intraoral 3d digital scanners for restorative dentistry. *Internet J Med Technol., 5*, http://archive.ispub.com/journal/the-internet-journal-of-medical-technology/volume-5-number-1/a-comparative-analysis-of-intraoral-3d-digital-scanners-for-restorative-dentistry.html - sthash.RBKUoHLw.dpbs. (Accessed June 21, 2013).

Logozzo, S., Zanetti, E. M., Franceschini, G., Kilpelä, A., & Mäkynen, A. (2013). Recent advances in dental optics - Part I: 3D intraoral scanners for restorative dentistry. *Opt Laser Eng,* http://dx.doi.org/10.1016/j.optlaseng.2013.07.017.

Lutz, F., Krejci, I., & Mormann, W. (1987). [Tooth-colored posterior restoration]. *Phillip J Restaur Zahnmed, 4*(3), 127-137.

Ma, T., Nicholls, J. I., & Rubenstein, J. E. (1997). Tolerance measurements of various implant components. *Int J Oral Maxillofac Implants, 12*(3), 371-375.

Mada, S. K., Smith, M. L., Smith, L. N., & Midha, P. S. (2003). Title: Overview of passive and active vision techniques for hand-held 3D data acquisition. *Proceedings of SPIE - the International Society for Optical Engineering*, 16-27.

Malo, P., de Araujo Nobre, M., Lopes, A., Francischone, C., & Rigolizzo, M. (2012). "All-on-4" immediate-function concept for completely edentulous maxillae: a clinical report on the medium (3 years) and long-term (5 years) outcomes. *Clin Implant Dent Relat Res, 14 Suppl 1*, e139-150.

Malo, P., Rangert, B., & Nobre, M. (2003). "All-on-Four" immediate-function concept with Branemark System implants for completely edentulous mandibles: a retrospective clinical study. *Clin Implant Dent Relat Res, 5 Suppl 1*, 2-9.

Martinez-Rus, F., Garcia, C., Santamaria, A., Ozcan, M., & Pradies, G. (2013). Accuracy of definitive casts using 4 implant-level impression techniques in a scenario of multi-implant system with different implant angulations and subgingival alignment levels. *Implant Dent, 22*(3), 268-276.

Mehl, A., Ender, A., Mormann, W., & Attin, T. (2009). Accuracy testing of a new intraoral 3D camera. *Int J Comput Dent, 12*(1), 11-28.

Mehl, A., Gloger, W., Kunzelmann, K. H., & Hickel, R. (1997). A new optical 3-D device for the detection of wear. *J Dent Res, 76*(11), 1799-1807.

Micheelis, W., & Schiffner, U. (2006). Vierte Deutsche Mundgesundheitsstudie (DMS IV). Ergebnisse zu oralen Erkrankungsprävalenzen, Risikogruppen und zum zahnärztlichen Versorgungsgrad in Deutschland 2005. In: (IDZ) IdDZ, ed. Vol. Materialienreihe Band 31 Deutscher Zahnärzte Verlag DÄV. Köln. 1-502.

Mojon, P., Oberholzer, J. P., Meyer, J. M., & Belser, U. C. (1990). Polymerization shrinkage of index and pattern acrylic resins. *J Prosthet Dent, 64*(6), 684-688.

Moreno, A., Gimenez, B., Ozcan, M., & Pradies, G. (2013). A clinical protocol for intraoral digital impression of screw-retained CAD/CAM framework on multiple implants based on wavefront sampling technology. *Implant Dent, 22*(4), 320-325.

Mormann, W. H., & Brandestini, M. (1987). [Cerec-System: computerized inlays, onlays and shell veneers]. *Zahnarztl Mitt, 77*(21), 2400-2405.

Mormann, W. H., Brandestini, M., & Lutz, F. (1987). [The Cerec system: computer-assisted preparation of direct ceramic inlays in 1 setting]. *Quintessenz, 38*(3), 457-470.

Mpikos, P., Kafantaris, N., Tortopidis, D., Galanis, C., Kaisarlis, G., & Koidis, P. (2012). The effect of impression technique and implant angulation on the impression accuracy of external- and internal-connection implants. *Int J Oral Maxillofac Implants, 27*(6), 1422-1428.

Nedelcu, R. G., & Persson, A. S. (2014). Scanning accuracy and precision in 4 intraoral scanners: an in vitro comparison based on 3-dimensional analysis. *J Prosthet Dent, 112*(6), 1461-1471.

NilsMalmgrenAB. (2015). Epoxy plastics' general chemical and physical properties. http://www.nilsmalmgren.com/epoxy-chemistry/epoxy-plastics-general-chemical-and-physical-properties/.

Ongul, D., Gokcen-Rohlig, B., Sermet, B., & Keskin, H. (2012). A comparative analysis of the accuracy of different direct impression techniques for multiple implants. *Aust Dent J, 57*(2), 184-189.

Optical Gaging Products Inc. (2015). http://www.ogpnet.com/north-america/systems/accuracy.

Papaspyridakos, P., Chen, C. J., Gallucci, G. O., Doukoudakis, A., Weber, H. P., & Chronopoulos, V. (2014). Accuracy of implant impressions for partially and completely edentulous patients: a systematic review. *Int J Oral Maxillofac Implants, 29*(4), 836-845.

Papaspyridakos, P., Gallucci, G. O., Chen, C. J., Hanssen, S., Naert, I., & Vandenberghe, B. (2015). Digital versus conventional implant impressions for edentulous patients: accuracy outcomes. *Clin Oral Implants Res*.

Patzelt, S. B., Bahat, O., Reynolds, M. A., & Strub, J. R. (2014). The all-on-four treatment concept: a systematic review. *Clin Implant Dent Relat Res, 16*(6), 836-855.

Patzelt, S. B., Bishti, S., Stampf, S., & Att, W. (2014). Accuracy of computer-aided design/computer-aided manufacturing-generated dental casts based on intraoral scanner data. *J Am Dent Assoc, 145*(11), 1133-1140.

Patzelt, S. B., Emmanouilidi, A., Stampf, S., Strub, J. R., & Att, W. (2014). Accuracy of full-arch scans using intraoral scanners. *Clin Oral Investig, 18*(6), 1687-1694.

Patzelt, S. B., Lamprinos, C., Stampf, S., & Att, W. (2014). The time efficiency of intraoral scanners: an in vitro comparative study. *J Am Dent Assoc, 145*(6), 542-551.

Patzelt, S. B., Vonau, S., Stampf, S., & Att, W. (2013). Assessing the feasibility and accuracy of digitizing edentulous jaws. *J Am Dent Assoc, 144*(8), 914-920.

Penarrocha-Oltra, D., Agustin-Panadero, R., Bagan, L., Gimenez, B., & Penarrocha, M. (2014). Impression of multiple implants using photogrammetry: description of technique and case presentation. *Med Oral Patol Oral Cir Bucal, 19*(4), e366-371.

Pozzi, A., Tallarico, M., Mangani, F., & Barlattani, A. (2013). Different implant impression techniques for edentulous patients treated with CAD/CAM complete-arch prostheses: a randomised controlled trial reporting data at 3 year post-loading. *Eur J Oral Implantol, 6*(4), 325-340.

Pujari, M., Garg, P., & Prithviraj, D. R. (2014). Evaluation of accuracy of casts of multiple internal connection implant prosthesis obtained from different impression materials and techniques: an in vitro study. *J Oral Implantol, 40*(2), 137-145.

Reich, S., Vollborn, T., Mehl, A., & Zimmermann, M. (2013). Intraoral optical impression systems--an overview. *Int J Comput Dent, 16*(2), 143-162.

Richter, E. J. (1998). In vivo horizontal bending moments on implants. *Int J Oral Maxillofac Implants, 13*(2), 232-244.

Rutkunas, V., & Ignatovic, J. (2014). A technique to splint and verify the accuracy of implant impression copings with light-polymerizing acrylic resin. *J Prosthet Dent, 111*(3), 254-256.

Sahin, S., & Cehreli, M. C. (2001). The significance of passive framework fit in implant prosthodontics: current status. *Implant Dent, 10*(2), 85-92.

Sahin, S., Cehreli, M. C., & Yalcin, E. (2002). The influence of functional forces on the biomechanics of implant-supported prostheses--a review. *J Dent, 30*(7-8), 271-282.

Saman, D. M., Lemieux, A., Arevalo, O., & Lutfiyya, M. N. (2014). A population-based study of edentulism in the US: does depression and rural residency matter after controlling for potential confounders? *BMC Public Health, 14*, 65.

Schepke, U., Meijer, H. J., Kerdijk, W., & Cune, M. S. (2015). Digital versus analog complete-arch impressions for single-unit premolar implant crowns: Operating time and patient preference. *J Prosthet Dent*.

Schulte, W. (1995). Implants and the periodontium. *Int Dent J, 45*(1), 16-26.

Schwarz, M. S. (2000). Mechanical complications of dental implants. *Clin Oral Implants Res, 11 Suppl 1*, 156-158.

Seelbach, P., Brueckel, C., & Wostmann, B. (2013). Accuracy of digital and conventional impression techniques and workflow. *Clin Oral Investig, 17*(7), 1759-1764.

Tan, K. B., Rubenstein, J. E., Nicholls, J. I., & Yuodelis, R. A. (1993). Three-dimensional analysis of the casting accuracy of one-piece, osseointegrated implant-retained prostheses. *Int J Prosthodont, 6*(4), 346-363.

van der Meer, W. J., Andriessen, F. S., Wismeijer, D., & Ren, Y. (2012). Application of intra-oral dental scanners in the digital workflow of implantology. *PLoS One, 7*(8), e43312.

Vandeweghe, S., Vervack, V., Vanhove, C., Dierens, M., Jimbo, R., & De Bruyn, H. (2015). Accuracy of optical dental digitizers: an in vitro study. *Int J Periodontics Restorative Dent, 35*(1), 115-121.

Wachman, E. S., Niu, W., & Farkas, D. L. (1997). AOTF microscope for imaging with increased speed and spectral versatility. *Biophys J, 73*(3), 1215-1222.

Wee, A. G. (2000). Comparison of impression materials for direct multi-implant impressions. *J Prosthet Dent, 83*(3), 323-331.

Wee, A. G., Aquilino, S. A., & Schneider, R. L. (1999). Strategies to achieve fit in implant prosthodontics: a review of the literature. *Int J Prosthodont, 12*(2), 167-178.

Wenz, H. J., & Hertrampf, K. (2008). Accuracy of impressions and casts using different implant impression techniques in a multi-implant system with an internal hex connection. *Int J Oral Maxillofac Implants, 23*(1), 39-47.

Wismeijer, D., Mans, R., van Genuchten, M., & Reijers, H. A. (2014). Patients' preferences when comparing analogue implant impressions using a polyether impression material versus digital impressions (Intraoral Scan) of dental implants. *Clin Oral Implants Res, 25*(10), 1113-1118.

Yamamoto, E., Marotti, J., de Campos, T. T., & Neto, P. T. (2010). Accuracy of four transfer impression techniques for dental implants: a scanning electron microscopic analysis. *Int J Oral Maxillofac Implants, 25*(6), 1115-1124.

Zen, B. M., Soares, E. F., Rodrigues, M. A., Luthi, L. F., Consani, R. L., Mesquita, M. F., & Henriques, G. E. (2014). Comparison of different transfer impression techniques accuracy for osseointegrated implants. *J Oral Implantol*.

ZenduraDentalTeam. (2012). What's so special about Polyurethane? http://www.zenduradental.com/blogs/zenduradental/6395330-whats-so-special-about-polyurethane.

Zimmermann, M., Mehl, A., Mormann, W. H., & Reich, S. (2015). Intraoral scanning systems - a current overview. *Int J Comput Dent, 18*(2), 101-129.

11 Appendix

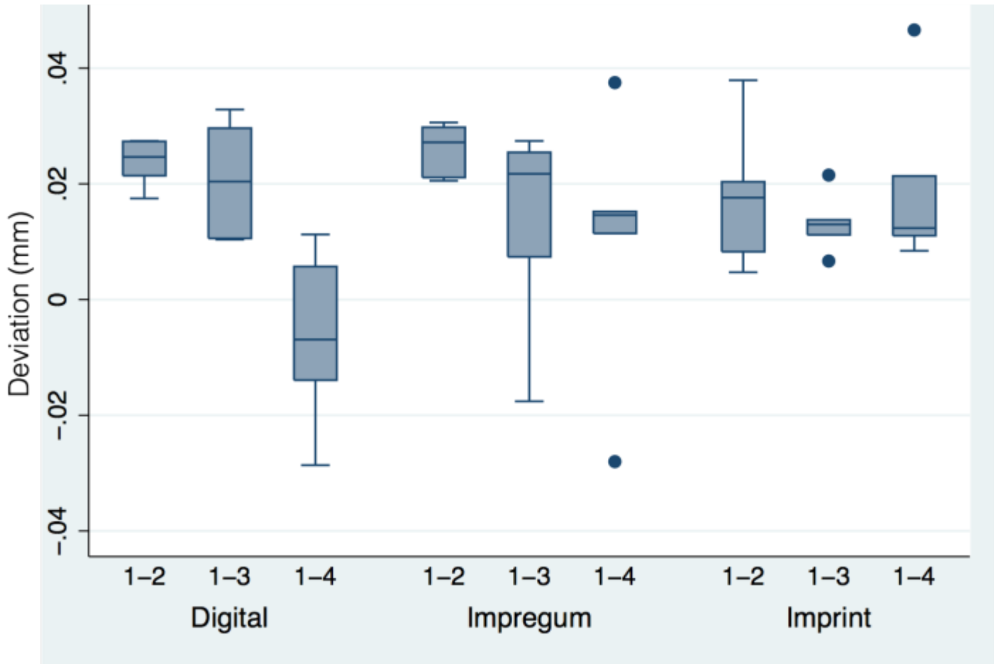

Figure 11-1: Boxplots representing the distance deviation of each impression-making group and each analyzed distance.

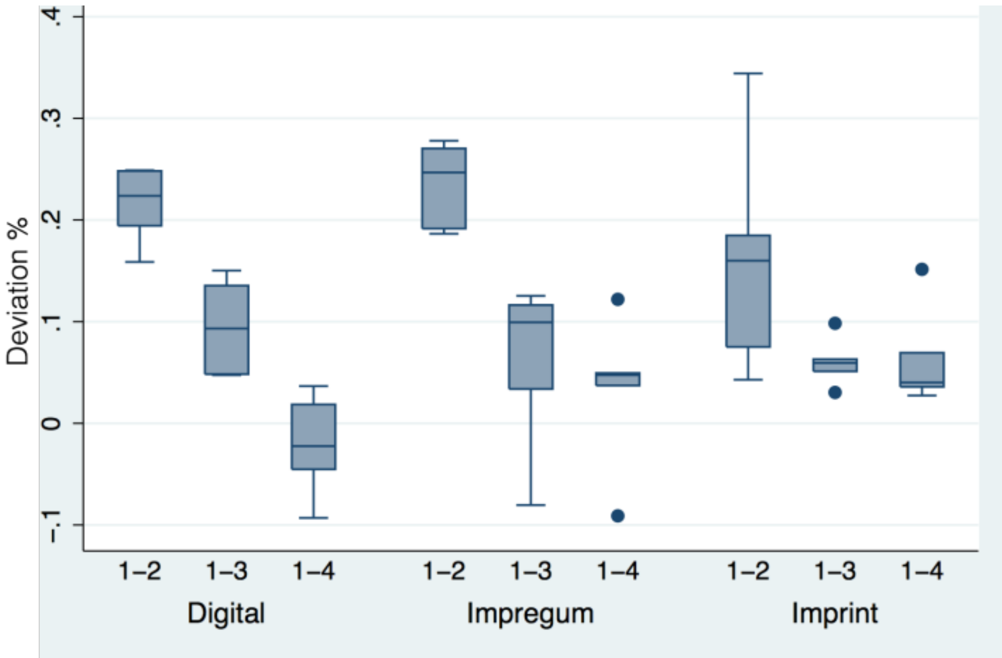

Figure 11-2: Boxplots representing the percentage expression of the distance deviation in each impression-making group and each analyzed distance.

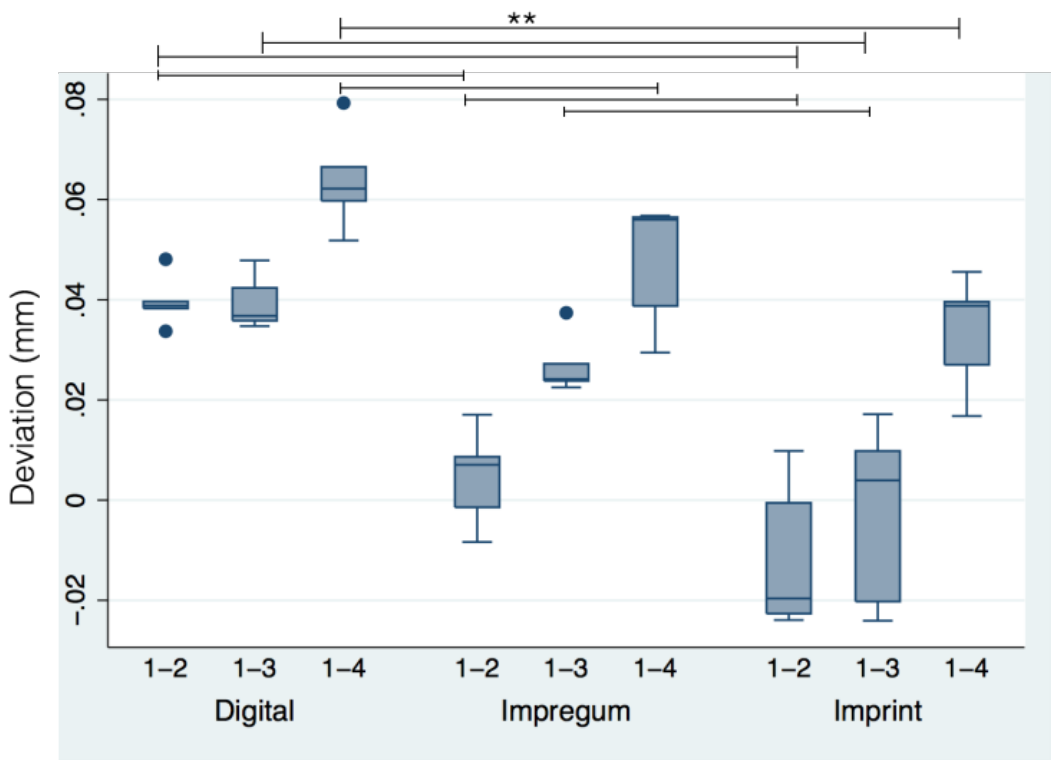

Figure 11-3: Boxplots representing the distance deviation of each impression-making group and each analyzed distance. Double asterisk: $p<0.05$ (in mean values).

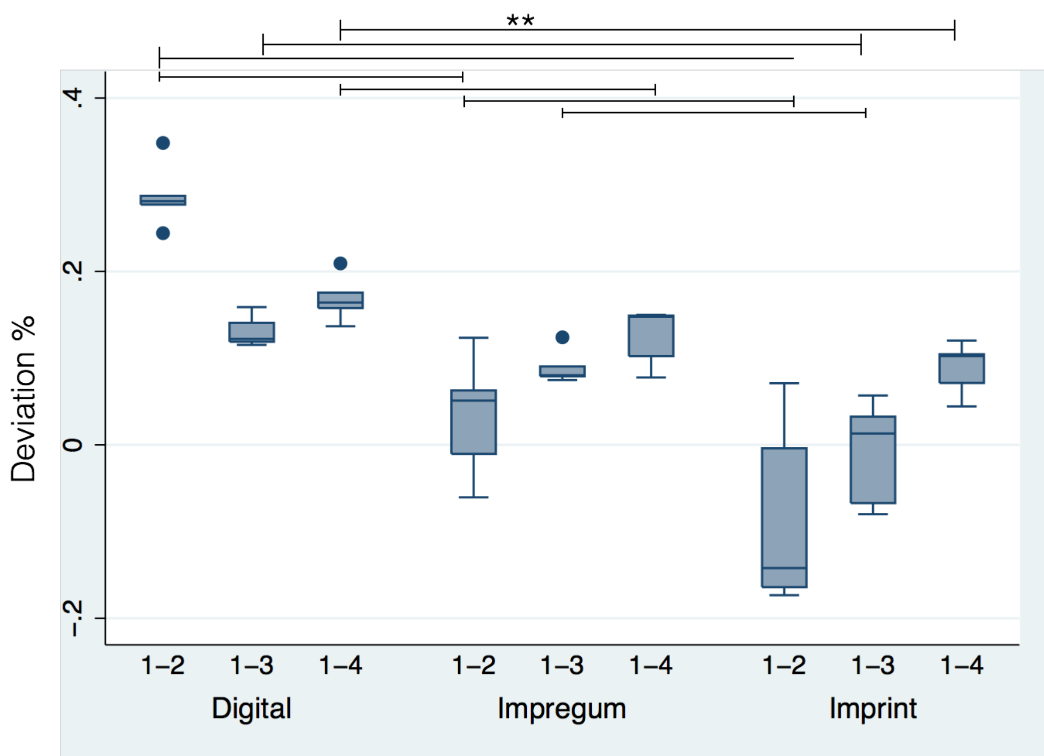

Figure 11-4: Boxplots representing the percentage expression of the distance deviation in each impression-making group and each analyzed distance. Double asterisk: $p<0.05$ (in mean values).

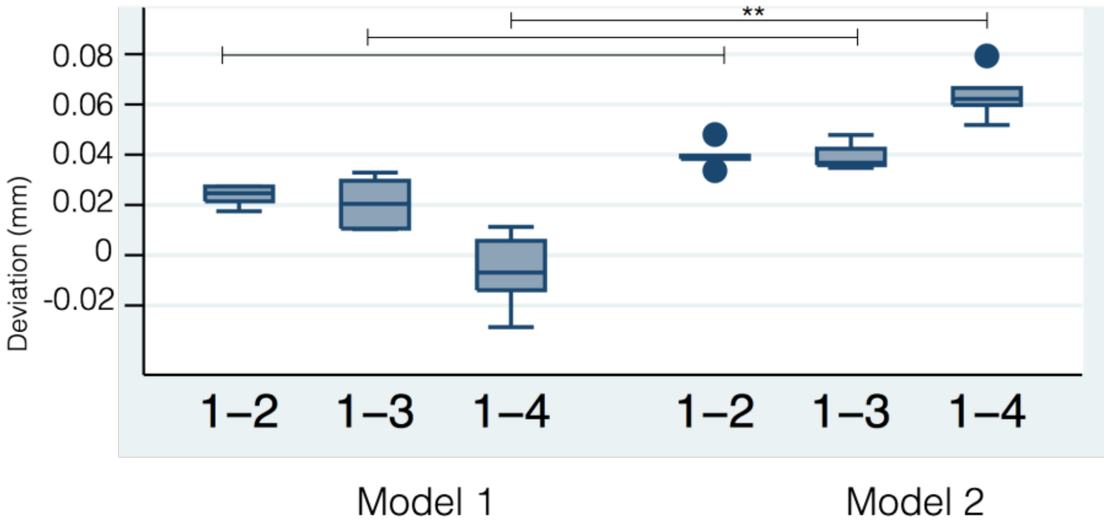

Figure 11-5: Boxplots representing the deviation of each analyzed distance for each reference model using the computer-aided impression-making method. Double asterisk: $p<0.05$ (in mean values).

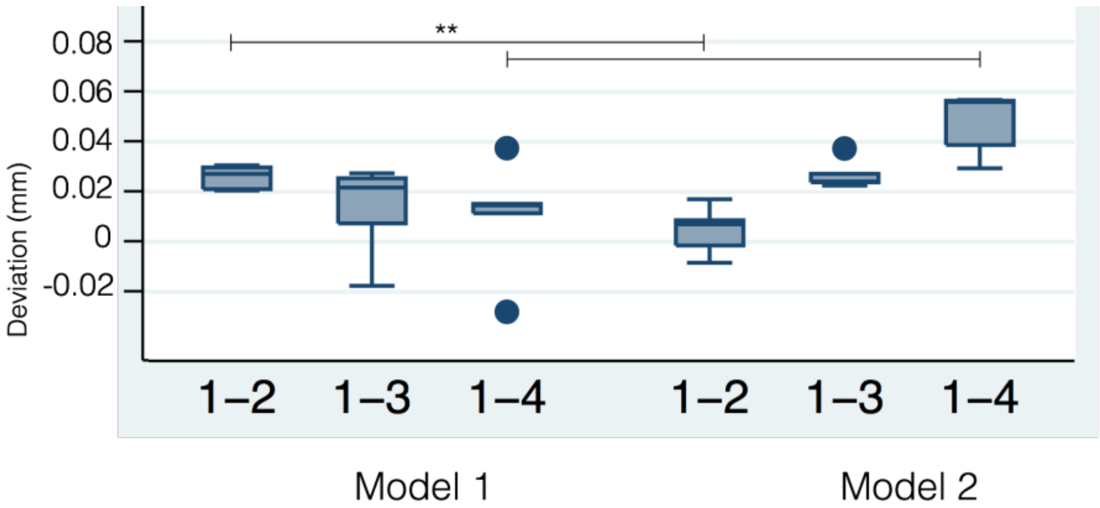

Figure 11-6: Boxplots representing the deviation of each analyzed distance for both reference models using conventional impression with Impregum. Double asterisk: $p<0.05$ (in mean values).

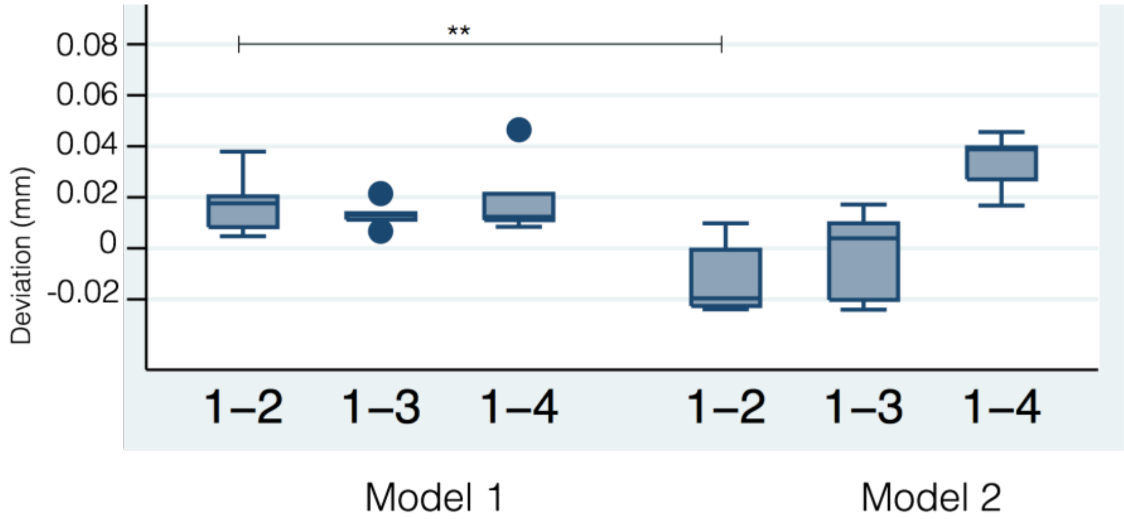

Figure 11-7: Boxplots representing the deviation of each analyzed distance for both reference models using conventional impression with Imprint. Double asterisk: p<0.05 (in mean values).

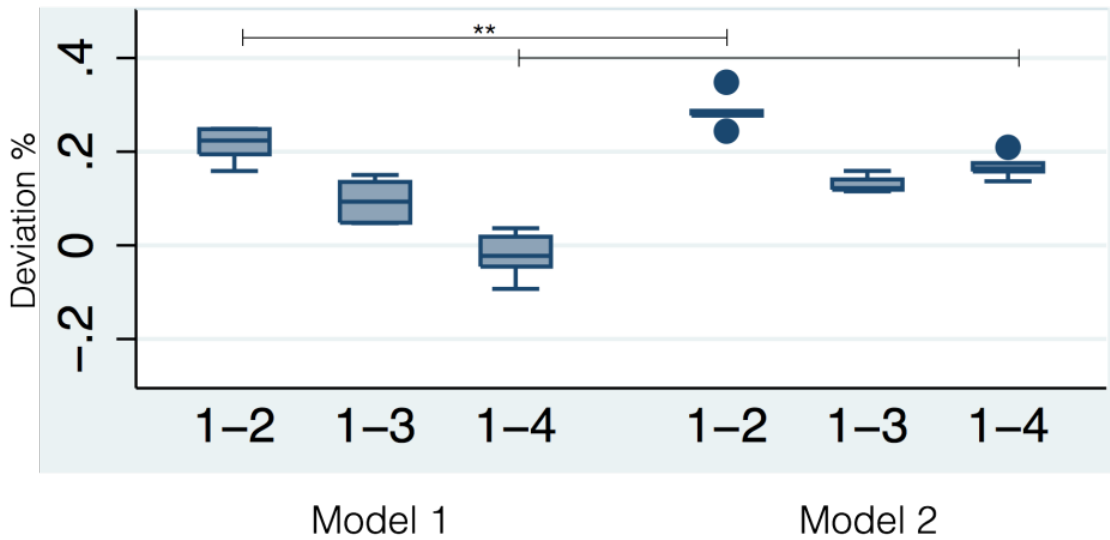

Figure 11-8: Boxplots representing the percentage expression of each analyzed distance deviation for both reference models using the computer-aided impression-making method. Double asterisk: p<0.05 (in mean values).

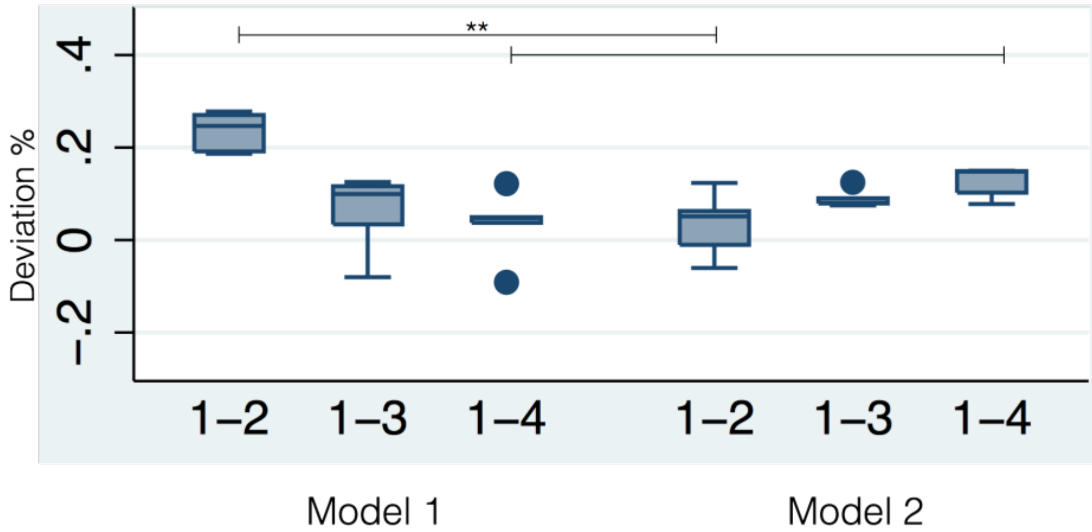

Figure 11-9: Boxplots representing the percentage expression of each analyzed distance deviation for both reference models using conventional impression with Impregum. Double asterisk: $p<0.05$ (in mean values).

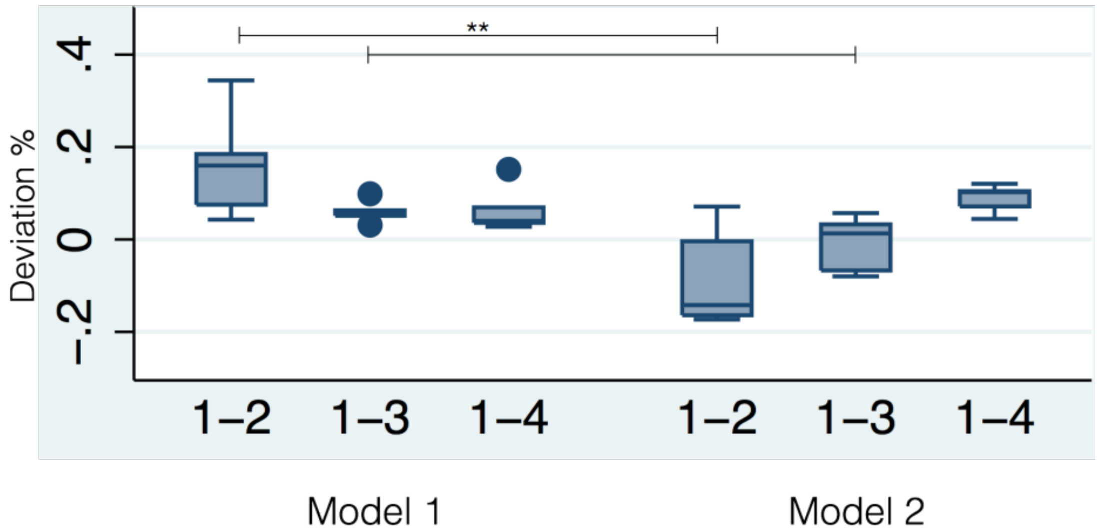

Figure 11-10: Boxplots representing the percentage expression of each analyzed distance deviation for both reference models using conventional impression with Imprint. Double asterisk: $p<0.05$ (in mean values).

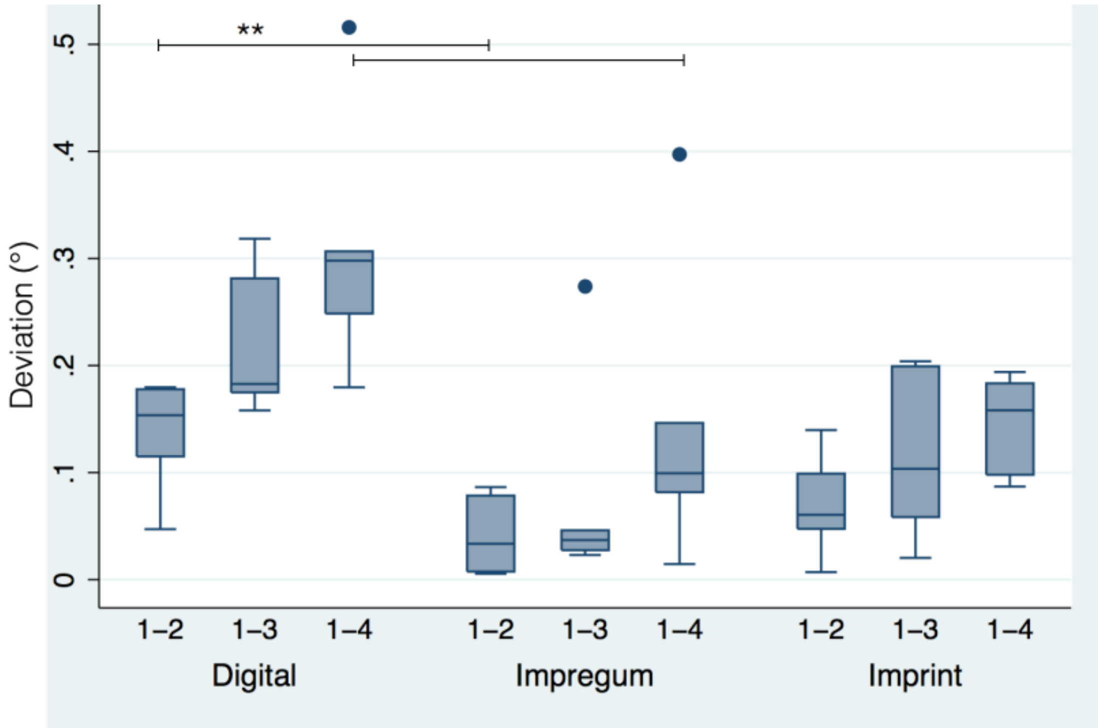

Figure 11-11: Boxplots representing the angle deviation of each impression-making group and each analyzed interval. Double asterisk: p<0.05 (in mean values).

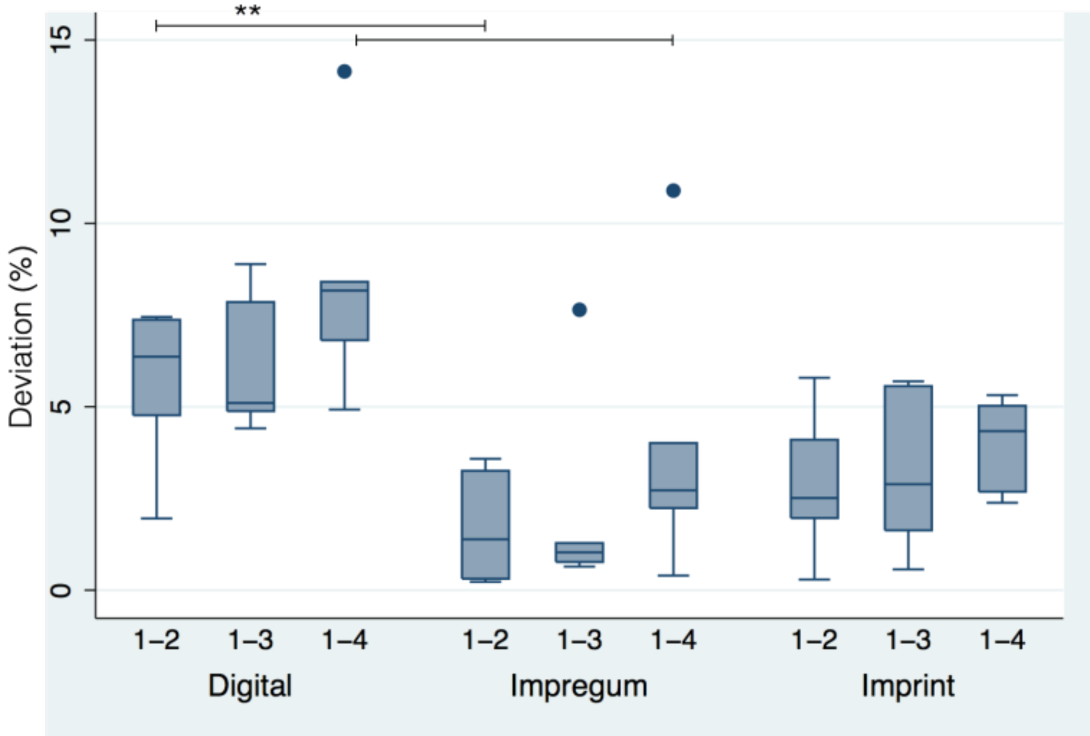

Figure 11-12: Boxplots representing the percentage expression of the angle deviation of each impression-making group and each analyzed interval. Double asterisk: p<0.05 (in mean values).

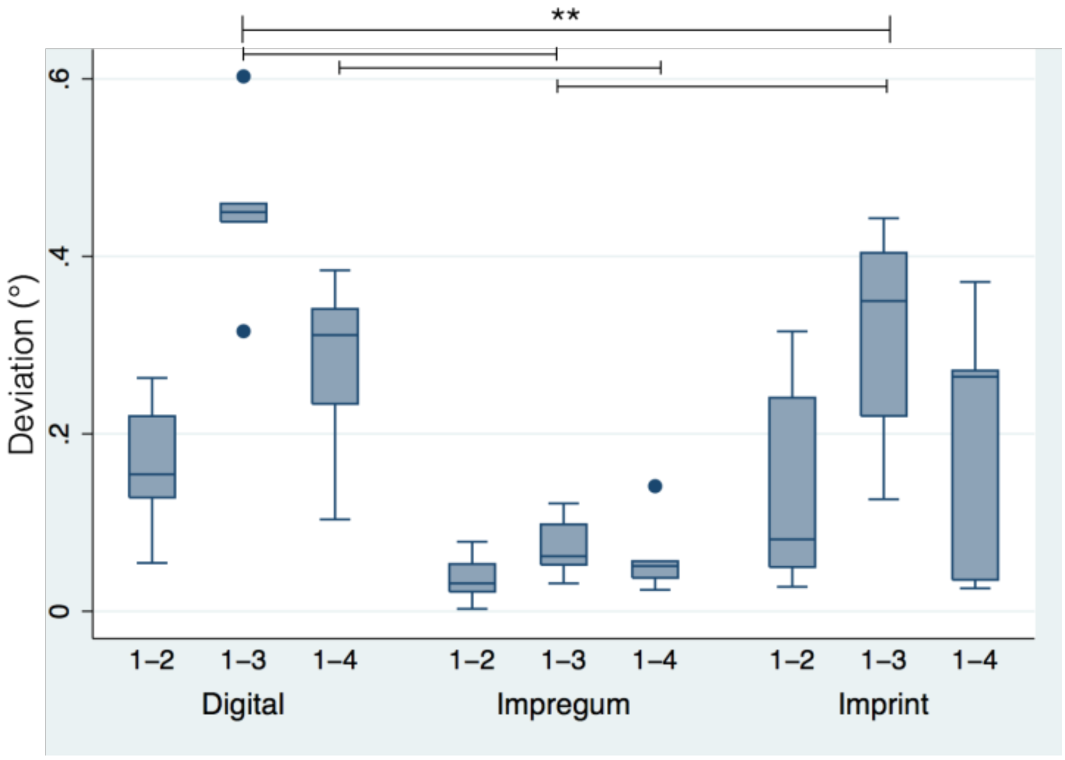

Figure 11-13: Boxplots representing the angle deviation of each impression-making group and each analyzed interval. Double asterisk: p<0.05 (in mean values).

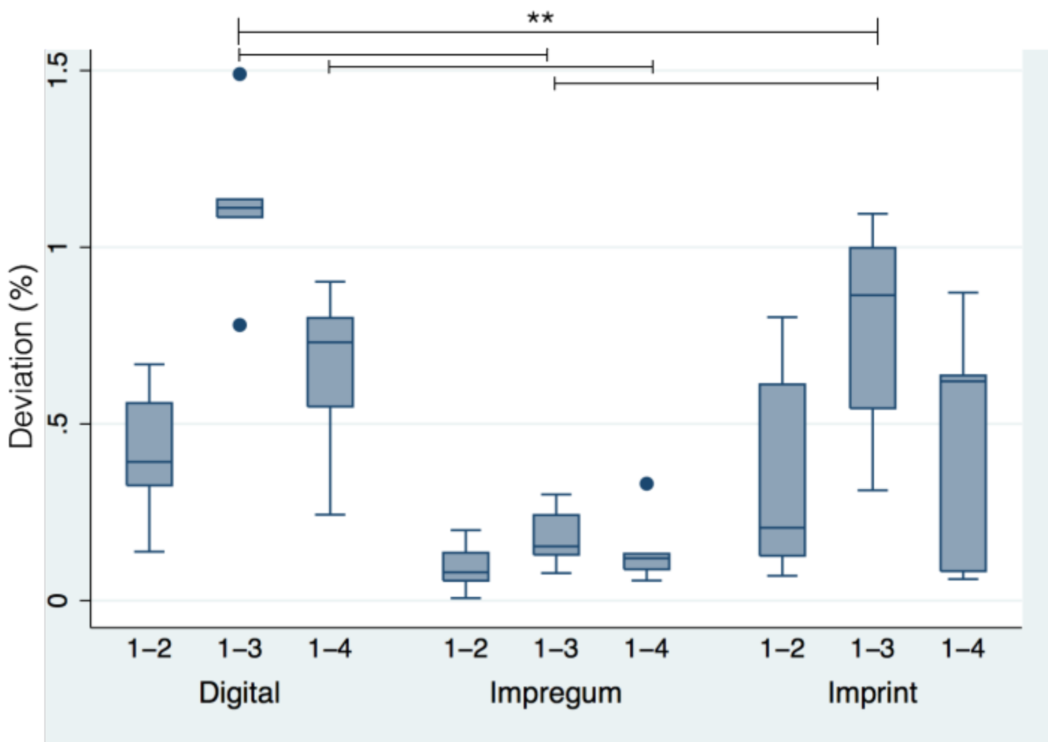

Figure 11-14: Boxplots representing the percentage expression of the angle deviation of each impression-making group and each analyzed interval. Double asterisk: p<0.05 (in mean values).

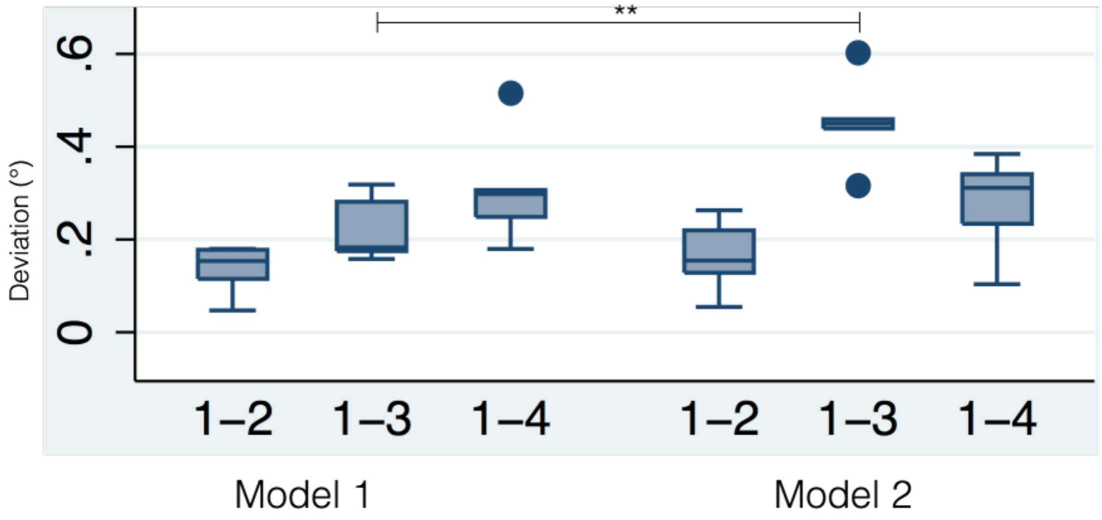

Figure 11-15: Boxplots representing the angle deviation from each reference model using the computer-aided impressing-making method. The deviation is given between the reference implant analog "1" and every further one ("2", "3", "4"). Double asterisk: p<0.05 (in mean values).

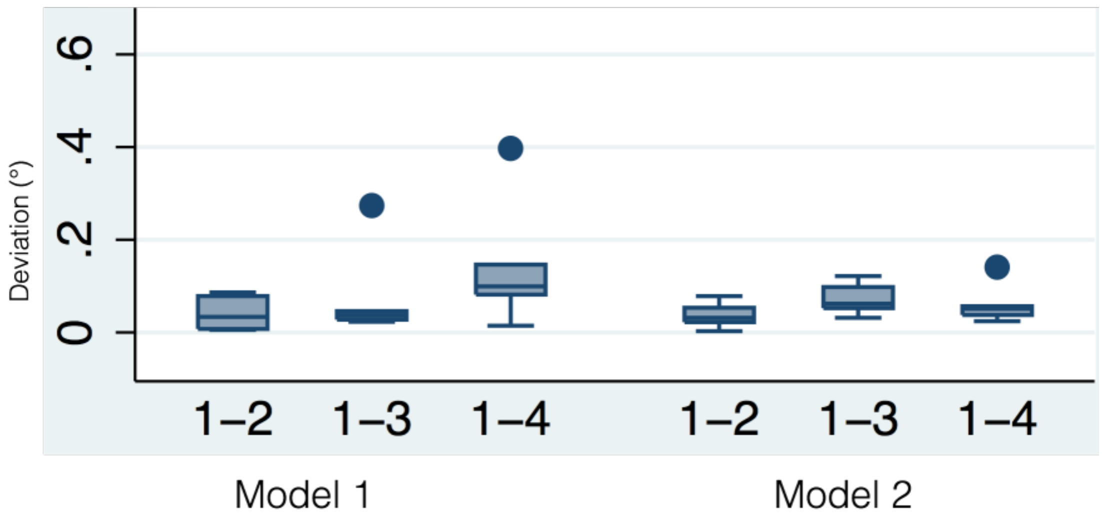

Figure 11-16: Boxplots representing the angle deviation from each reference model using the conventional impression-making method with Impregum. The deviation is given between the reference implant analog "1" and every further one ("2", "3", "4").

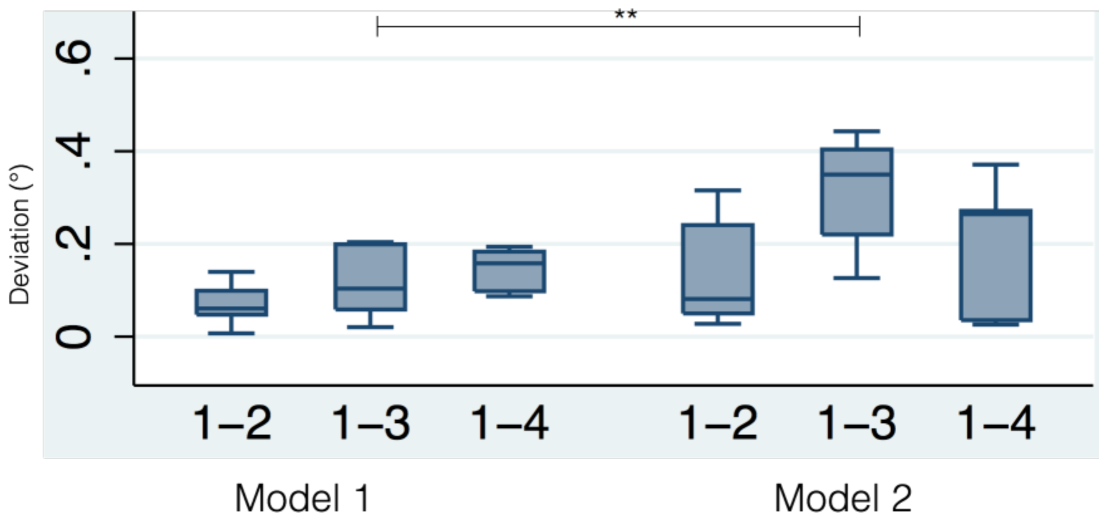

Figure 11-17: Boxplots representing the angle deviation from each reference model using the conventional impression-making method with Imprint. The deviation is given between the reference implant analog “1” and every further one (“2”, “3”, “4”). Double asterisk: p<0.05 (in mean values).

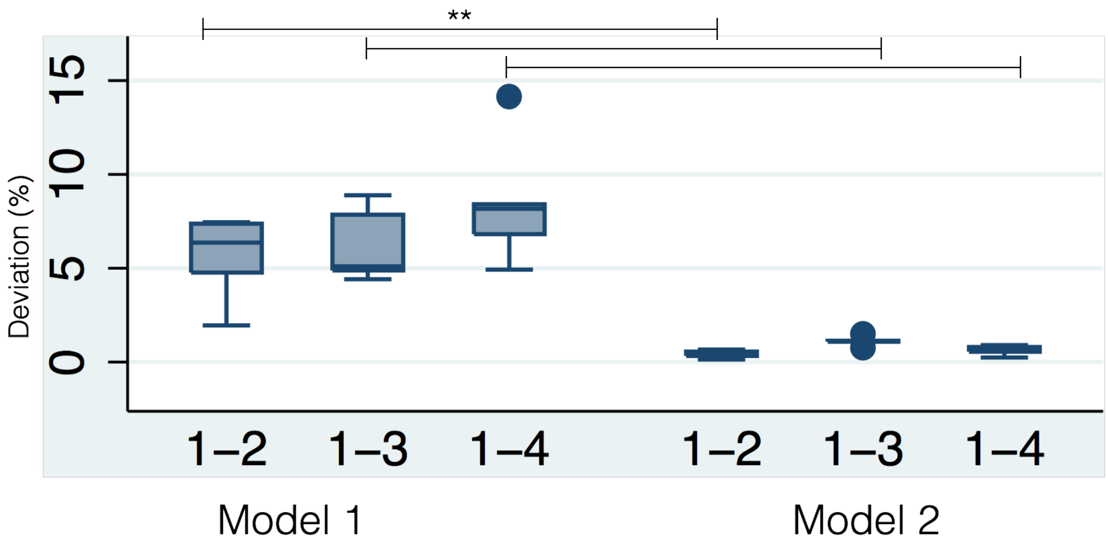

Figure 11-18: Boxplots representing the percentage expression of the angle deviation from each reference model using the computer-aided impression-making method. The deviation is given between the reference implant analog “1” and every further one (“2”, “3”, “4”). Double asterisk: p<0.05 (in mean values).

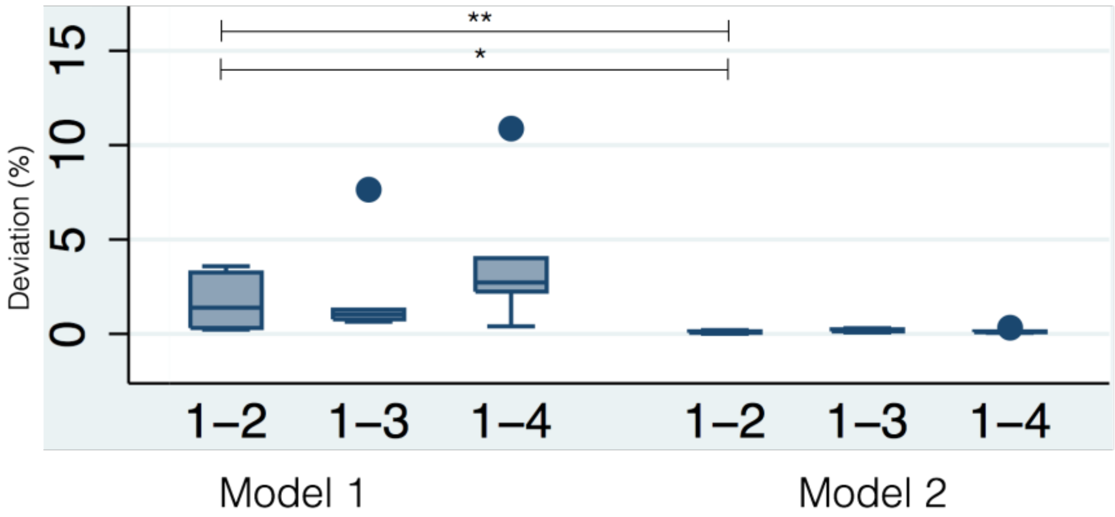

Figure 11-19: Boxplots representing the percentage expression of the angle deviation from each reference model using a conventional impression with Impregum . The deviation is given between the reference implant analog “1” and every further one (“2”, “3”, “4”). Asterisk: p<0.05 (in variability values), double asterisk: p<0.05 (in mean values).

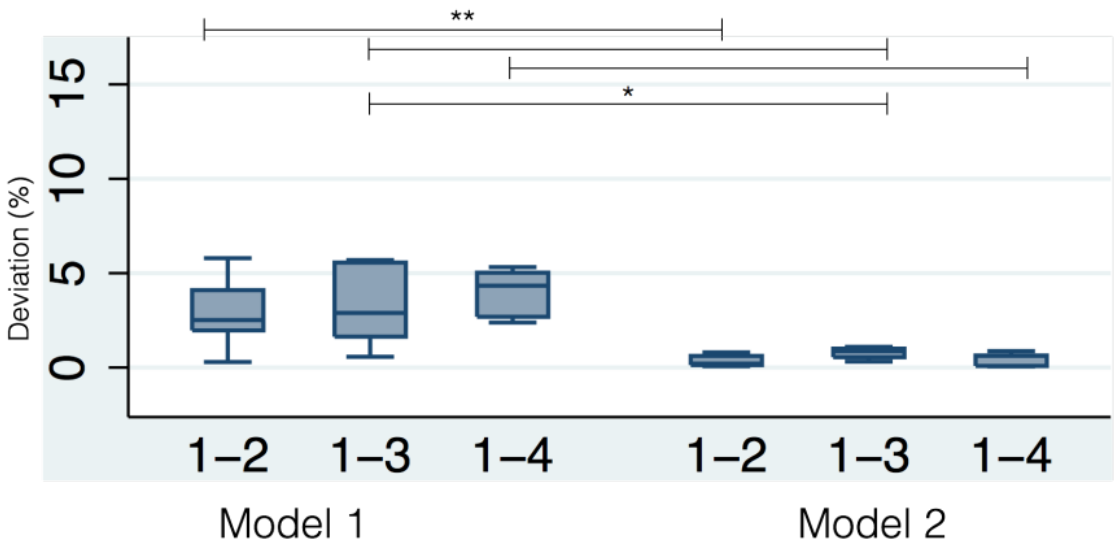

Figure 11-20: Boxplots representing the percentage expression of the angle deviation from each reference model using a conventional impression with Imprint. The deviation is given between the reference implant analog “1” and every further one (“2”, “3”, “4”). Asterisk: p<0.05 (in variability values), double asterisk: p<0.05 (in mean values).

12 Acknowledgements

First, I would like to thank Prof. Dr. Dr. h. c. J. R. Strub for giving me the opportunity to complete the postgraduate program and to write the doctoral thesis at his Department of Prosthodontics at the Albert-Ludwigs University in Freiburg.
I wish to express my sincere thanks and gratitude to the director of the postgraduate program and my supervisor Prof. Dr. W. Att. Thanks for your support and friendship throughout these years in Freiburg.
I would like to extend my special thanks and gratitude to Dr. S. B. M. Patzelt. I am very thankful for your availability, patience and strong guidance during writing my doctoral thesis.
I would also like to thank Mr. A. Alvarez for his help during the data analysis and Mrs. K. Vach for the preparation of the statistics.

My biggest thanks are assigned to Prof. K. Malament for his invaluable support and belief in me.

My sincere gratitude and appreciation go to my family. I would like to thank my mom Asta and my grandma Alma for their constant encouragement not only during the last years, but also during all my life. Thanks to my little brother Ainis for the continuous inspiration with his positive attitude. Special thanks to my dad Audris, who was always my friend and the coach of my personality.

I would like to dedicate my deepest and the most sincere gratitude to my husband Auris. I deeply appreciate your love, trust, invaluable support and continuous belief in me. Thanks for inspiring me and being the core of my life.